Annual Progress Report

ULI2 Step-B-0060, Composite Manufacturing Technologies for Aerospace Performance at Automotive Production Rates

Grant Number 80NSSC20M0164

Principal Investigator
John W. Gillespie Jr.
Center for Composite Materials
101 Academy Street
Newark, DE 19716

September 1, 2021 – August 31, 2022

NASA Technical Points of Contact
Koushik Datta, Koushik.Datta@nasa.gov
Dawn C. Jegley, dawn.c.jegley@nasa.gov

Report submitted to:
Technical Officer / Koushik Datta
NASA Ames Research Center
Moffett Field, CA 94035-1000

Grants Officer
NASA Shared Services Center
Procurement Office, Bldg 1111
Stennis Space Center, MS 39529
NSSC-Grant-Report@mail.nasa.gov

New Technology Representative
NASA Ames Research Center
Code 202A-3
Moffett Field, CA 94035-1000
kelly.l.garcia@nasa.gov

Executive Summary

The National Aeronautics and Space Administration (NASA) University Leadership Initiative selected a team led by the University of Delaware Center for Composite Materials (UD-CCM) to address technology barriers and education/workforce training needs in composites manufacturing technologies providing aerospace performance at automotive production rates for the Urban Air Mobility (UAM) and commercial air platforms. Our program is a 4-year effort. This Annual Progress report covers the second year of the program from September 1, 2021, to August 31, 2022. The progress report includes a summary of program highlights in the areas of research and education/workforce training.

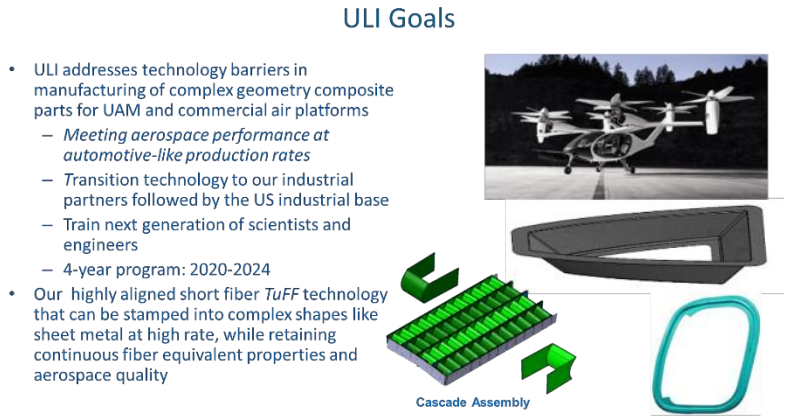

Our Team

Our team consists of UD-CCM as the lead organization with core team members from the composite supply chain from material suppliers, part manufacturers (ATC, Leach), and UAM and aerospace system integrator (Joby Aviation, John Geriguis & Spirit AeroSystems, Kerrick Dando). Our academic partner is Southern University SU (Patrick Mensah) who is actively involved in research and contributing to our education and outreach activities to underrepresented minorities from K-14 in aerospace applications of composites. Our outreach to other institutions is significant and include other academic and commercial entities.

Background on NASA Grand Challenge for UAM

Urban Air Mobility (UAM), a safe and efficient air transportation system for on-demand mobility (ODM) from small package delivery to air taxis, has arrived as the next frontier in air transportation. With NASA leading UAM efforts in identifying technical, operational challenges and regulatory frameworks, a community of small to large companies are investing significant resources into establishing infrastructure, digital frameworks, platforms, and operational models. Market studies[1] have established economic factors (estimated market size ~$500B, projected total number of air taxis exceed 850,000 in the US alone) with NASA setting forth a Grand Challenge. With higher production volumes and smaller size than commercial aircraft, studies have identified the need for next generation composite materials and manufacturing methods to meet ODM goals of affordability, safety, and lifecycle emissions. However, the maturity levels of today's manufacturing readiness[2] to achieve aerospace performance at automotive rates is ranked low. A NASA Roadmap in manufacturing and integrated structures[3] identified UAM technology for a 15-year timeframe with operational prototypes by 2026, and technology scaling by 2031. Flexible automated composite manufacturing methods were identified, in combination with integrated structure/material concepts for anti-ice, health monitoring etc. Similarly, commercial air platforms

have made the change to composites use for large structures (wings, fuselage etc.), but retain metal components for smaller, complex parts typical of the UAM vehicles.

Our Approach

Our project addresses these technology barriers in manufacturing of complex geometry composite parts for UAM and commercial air platforms by use our revolutionary highly aligned short fiber technology (called *TuFF* or Tailorable universal Feedstock for Forming) that can be formed into complex shapes like sheet metal at high rate, while retaining continuous fiber equivalent properties and aerospace quality. The novel material and manufacturing approach create a paradigm shift for manufacturing of commercial air and UAM vehicle structures.

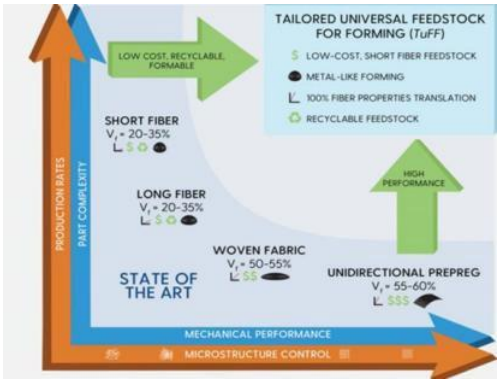

Under a 4-year DARPA-funded program (2017-2021) and an Office of Naval Research Defense University Research Instrumentation Program (ONR DURIP) Equipment Grant, UD-CCM has developed a pilot that aligns short fiber into preforms, creates prepreg by film infusion and includes a forming cell to produce formed parts at rate in one facility. This equipment is being used in our ULI program to make materials and parts identified by our team members. The site will also be used for training of Historically black colleges and universities (HBCU) faculty and students from Southern University and to conduct technology demonstrations for the UAM and aerospace supply chain.

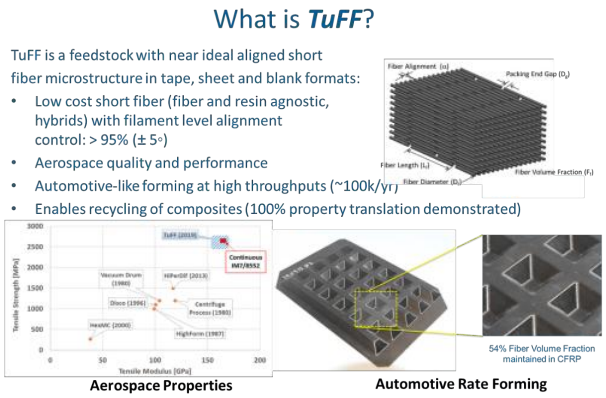

TuFF Integrated Manufacturing Facility

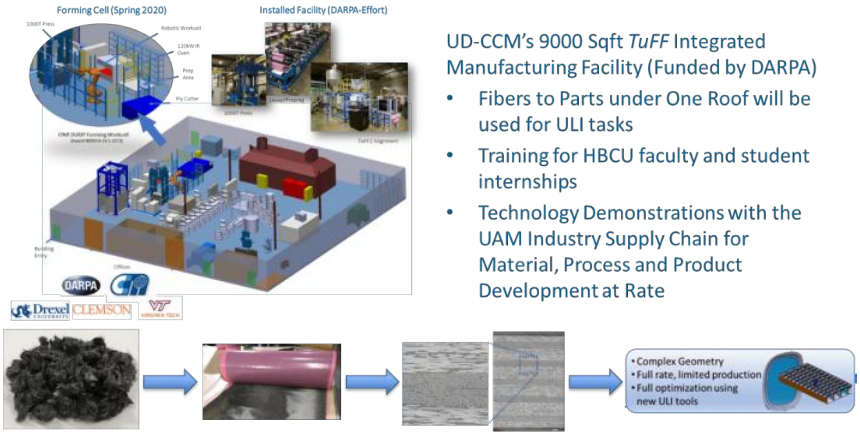

Our TuFF pilot-scale facility allows part manufacturing from short fibers under one roof

ULI Advisory Board and Meetings

An External Advisory Board (EAC) has been established to evaluate our ULI program progress. The chair of the Board is Mr. Mick Maher with over 30 years of experience in composites as former Program Director at Defense Advanced Research Projects Agency (DARPA) who ran the Open Manufacturing and Tailored Feedstock for Forming composite aerospace initiatives, Branch Chief of the Composites Branch at Army Research Lab (ARL) and worked in industry for decades. He has recruited additional board member from industry original equipment manufacturers (OEM) and the supply chain, academia, and the FAA. The board convenes during our annual program review (first year review was held on 10/20/21) and during our summer meeting (7/12/22) to provide verbal and written feedback.

ULI External Advisory Board
Board Chair: Michael Maher
Industry OEMs

- Spirit Representative: Kim Caldwell
- Joby Representative: John Geriguis

Academia

- Prof. Shridhar Yarlagadda (UD-CCM liaison)
- Prof. Srikanth Pilla (Clemson)
- Prof. Jim Sherwood (UMass)

FAA: Curt Davies

"Excellent fundamental work on understanding how the new material format behaves"

"Along with the breadth, the technical depth was seen as being very impressive"

- Selected comments from the ULI EAC

In terms of meetings, we have weekly internal meeting with task leads, monthly meetings with our external team members, monthly technical meetings with NASA (organized by Dawn Jegley and Kaushik Datta) and semi-annual meetings with our external board.

Education, Workforce, Outreach and Diversity Highlights

During the past year, we have been very active in education/workforce training and outreach to involve students including underrepresented minorities in composites activities at UD and SU. Overall, approximately 550 students (60% were URM from grades K-12) were involved and more than 450 people registered for presentations and seminars co-sponsored by our ULI. In addition, more than 1000 people in total registered for the 2022 NASA ImaginAviation Annual Conference and NASA Tech Talk Seminar series that highlighted our ULI students and technical activities.

With respect to Diversity, our ULI funded 14 PI/Co-PI's (14% Underrepresented Minorities (URM)) and 20 students/post-doctoral researcher. An additional 61 students (unfunded) benefited from ULI activities. Within this student group 16% were URM and 15% female. Additional details are given in the Diversity section below.

Technical Highlights

Our ULI program is organized into eight technical tasks and our Education/Workforce Training and Outreach Activities. The technical highlights and publications are provided in this section. Educational/Workforce Training and Outreach highlights are presented in the next section. Details on diversity are provided in the appendix.

The science base for microstructural design of *TuFF* composites during the alignment process and the influence of the microstructure on forming characteristics and mechanical properties of *TuFF* composites does not yet exist for this new technology. To establish the science base, we are developing a computational multi-scale framework for material selection of the constituents and micromechanics model for the prediction of anisotropic constitutive models for viscosity for forming simulations of complex geometry parts and micromechanics model for prediction of static and fatigue properties of the materials. Our overall vision is to leverage commercial software for CAD/CAM/CAE for composites and integrate the key results (material models and material databases) through custom development subroutines (UMATs) to enable design of materials, forming processes and part design using *TuFF* composites.

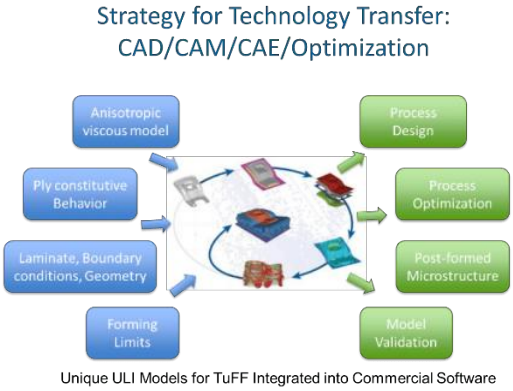

Unique ULI Models for TuFF Integrated into Commercial Software

ULI technical tasks will create the science-base for microstructural design of TuFF composites

The specific technical tasks are:

1) Materials and Part Selection
2) Micromechanics of Aligned Short Fiber Composites
3) Physics of Fiber Alignment
4) Micromechanics of Anisotropic Viscosity, Constitutive Model Development and Forming Limits
5) Process Development
6) Self-Healing Composites

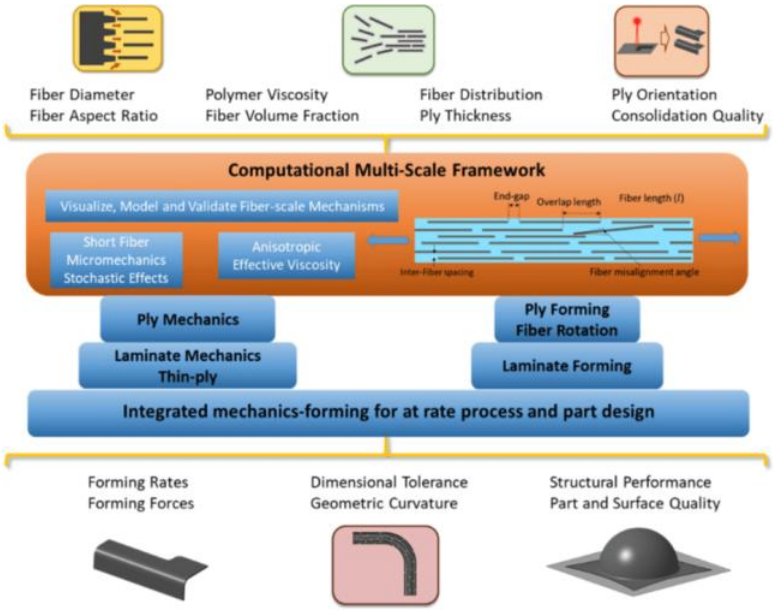

Highlight: Materials and Part Selection

In discussions with industry team members, various parts have been selected by Joby and Spirit Aerospace ranging from doors and instrument panels for the UAM platform to thrust reverser cascade for aircraft that are particularly difficult to manufacture with continuous fiber composites and are well suited to demonstrate the formability of *TuFF* composites. Down selection of parts will occur in Year 3 of our program. Current carbon fibers of interest include intermediate (IM7, T800) and standard modulus (AS4 and T700) carbon fiber. Currently Hexcel IM7 and AS4 are readily available as unsized fibers which is desired for use with engineering thermoplastic matrices that process at high temperatures. Low-melt polyaryletherketone (LM-PAEK) sourced from Victrex was chosen as the thermoplastic matrix for our program. This matrix is a semicrystalline thermoplastic with excellent solvent resistance and fracture toughness and the advantage of lower process temperature ("low melt") than other candidate systems. LM-PAEK AE250 grade film in 60- and 200-micron thickness has been received and is being used to product IM7/LM-PAEK prepreg with 3mm aligned short fibers (aspect ratio of 600).

Proposed candidate parts supplied by Joby

- Spirit has identified a Thrust Reverser Cascade as a candidate part
  - Thermoplastic stamp forming of TuFF composite for cascade components
    - 24 cascades per airplane, 50 vanes per cascade
    - 1200 vanes per aircraft, 2 geometries (600 each)

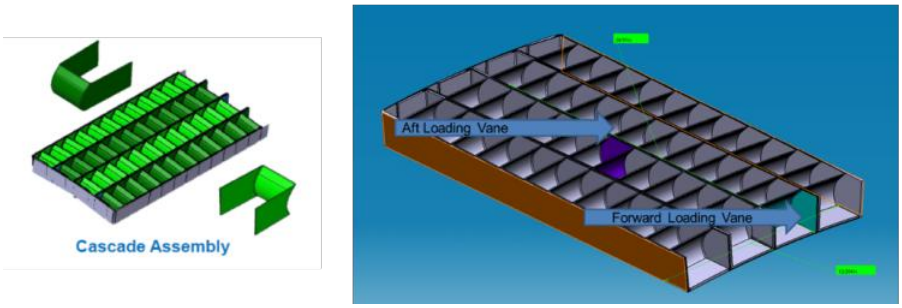

Proposed candidate parts supplied by Spirit Aerospace

To achieve aerospace level of mechanical properties with aligned short fibers, it is essential to achieve excellent fiber alignment within the preform (i.e., 95% of the fibers within the preform are aligned within +-5°). This is required to enable high fiber volume fraction (57%) during prepreg manufacturing to be achieved. Fiber breakage during the alignment process must also be minimized to retain unimodal fiber length distribution (see project on Physics of Fiber Alignment below). In addition, high levels of interfacial bonding between the unsized carbon fiber and the

LM-PAEK is required. In our past work with IM7/polyetherimide an interfacial shear strength exceeding 60 MPA is required to achieve properties equivalent to continuous fiber composites. Last year, single fiber pull-out experiments with an embedded length of 50 microns provided and outstanding level of bonding between IM7 and LM-PAEK with an Interfacial Shear Strength (IFSS) of 128.7 +- 20 MPa.

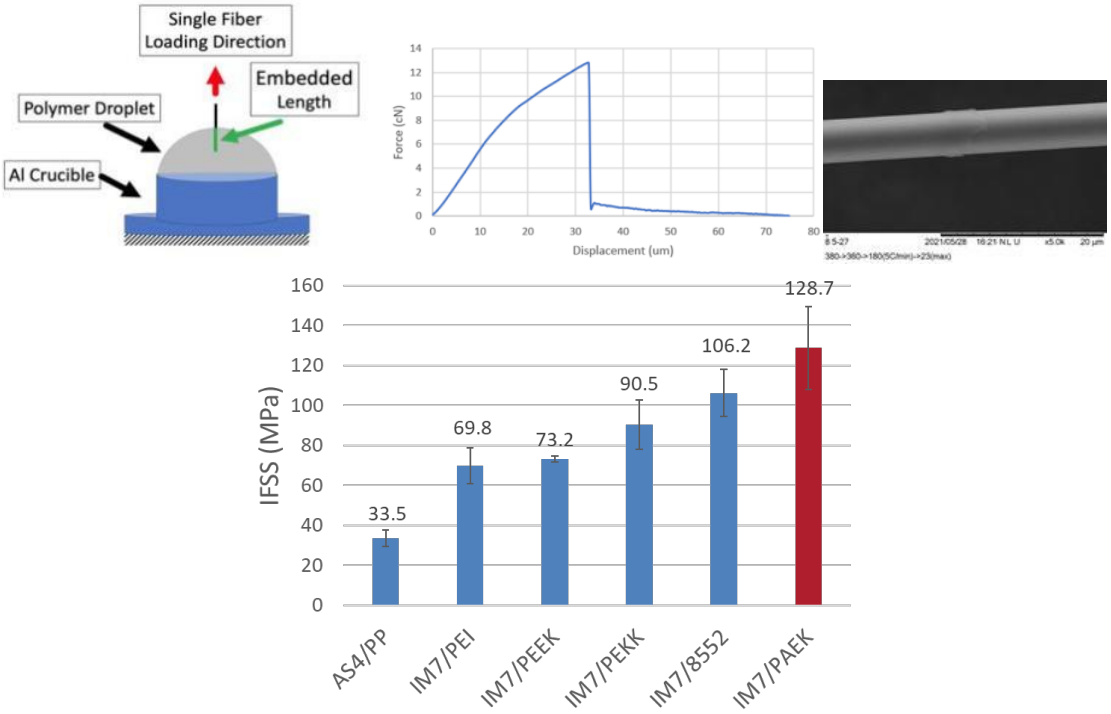

Excellent interfacial bonding is required with short fibers for full composite property translation

Unidirectional panels were fabricated using 3mm IM7/LM-PAEK for tension testing. Nominal 120 gsm fiber areal weight per ply preform was resin film infused using the 60-micron film to yield a fiber volume fraction (FVF) of ~54%. One of the challenges in making high quality panels was formation of wrinkles/waviness in the fiber that reduce tensile and compressive properties of the composite. LM-PAEK at processing temperatures has lower viscosity than PEI thermoplastics and as a semicrystalline polymer undergoes resin shrinkage. The origin of wavy fibers was visualized using novel experiments on single fibers with model thermoplastic polymers (see our project on micromechanics of aligned fibers). Based on these results high performance panels without wrinkles were fabricated for static and fatigue testing of the composite.

Excellent strength (325+-15Ksi) and modulus (21.5+-0.4Msi) data is achieved with low coefficients of variation of 4.7% and 1.7%, respectively. Strain to failure in the fiber direction is 1.45%. The National Institute for Aviation Research (NIAR) database for continuous fiber IM7/8552 at 58% FVF is a point of comparison for our aligned short fiber *TuFF* composites. Normalizing our results to 58% FVF gives a tensile strength of 349 Ksi and modulus of 23Msi which is very close to the continuous fiber tensile strength (363Ksi) and modulus (23Msi).

Sample #	Width (in.)	Thickness (in.)	Area (in^2)	P^{MAX} (Lbf)	Strength (Ksi)	Modulus (Msi)	Poissons Ratio	%Strain
1	0.4907	0.0189	0.0093	2979	321.55	21.36	0.34	1.46E-02
2	0.4902	0.0187	0.0092	2678	291.83	21.29	0.36	1.33E-02
3	0.4857	0.0187	0.0091	2940	324.22	21.30	0.37	1.45E-02
4	0.4947	0.0185	0.0092	3041	331.74	21.91	0.38	1.47E-02
5	0.4860	0.0186	0.0090	2954	326.43	20.93	0.32	1.50E-02
6	0.4920	0.0187	0.0092	3180	346.01	21.85	0.36	1.52E-02
7	0.4908	0.0186	0.0091	3037	332.14	21.92	0.36	1.45E-02
8	0.4903	0.0187	0.0092	2974	323.85	21.75	0.37	1.44E-02
Average					324.72	21.54	0.36	1.45%
St. Dev.					15.37	0.37	0.02	0.04%
					4.73%	1.70%		

Tension property evaluation with 3mm IM7/LM-PAEK

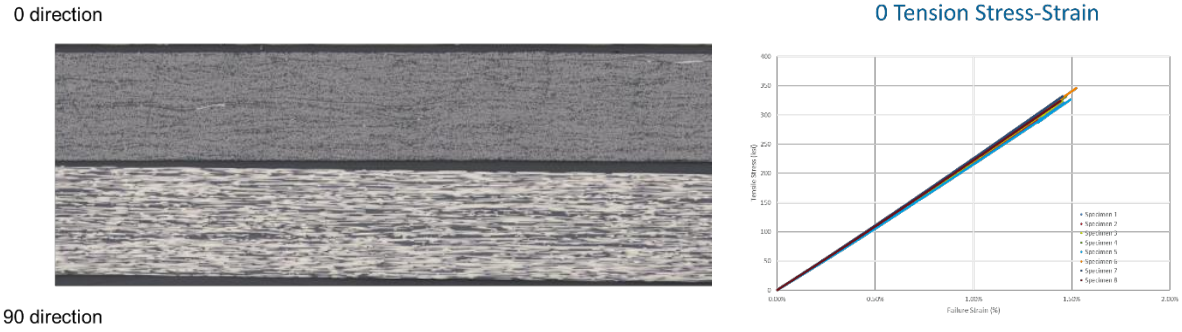

Another highlight related to mechanical properties was the continuation of our fatigue testing of unidirectional *TuFF* composites. Last year, IM7/PEI *TuFF* composites comprised of aligned 3mm carbon fibers at FVF of 57% was shown to be comparable to fatigue data in the literature for carbon fiber composites. This year, 3mm IM7/LM-PAEK unidirectional panels were tested using the same methodology. In this task, the SN curve for tension-tension fatigue (R=0.1) was conducted at three stress levels (85%, 75% and 50% of the mean-3 standard deviations). In all cases, no evidence of modulus reduction was measured. In addition, the samples were fatigue to 2 million cycles without failure (one 85% sample failed at 411,000 cycles due to a defect).

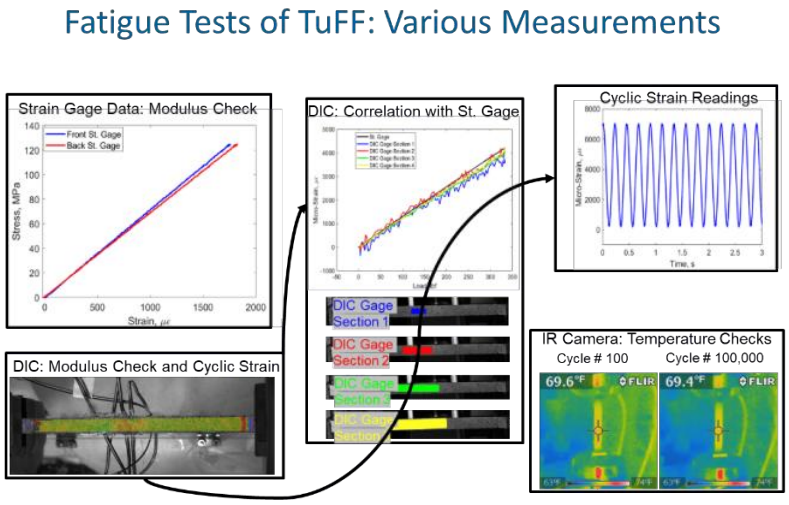

These results were far superior to last year's results on 3mm IM7/PEI *TuFF* samples. In fact, these results for 3mm IM7/LM-PAEK are superior to continuous fiber AS4/PEEK and both 3mm *TuFF* samples are far better than the continuous fiber AS4/epoxy. The high level of fatigue resistance of the 3mm *TuFF*/LM-PAEK may be attributed to the high level of interfacial adhesion reported above. Single fiber fatigue studies are planned to study effects of cycling loading on fiber/matrix debonding that could occur at the ends of the short fiber. This study on composite fatigue will continue in the coming year and will focus on fatigue testing of cross-ply laminates with thin ply layers to assess resistance to microcracking.

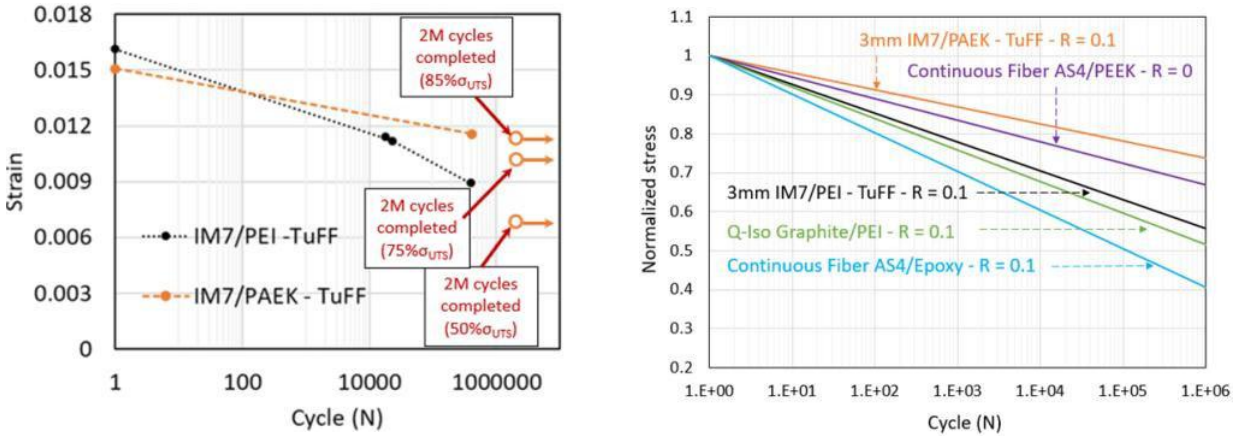

Highlights: Micromechanics of Aligned Short Fiber Composites

Continuum properties of *TuFF* composites (such as the static and fatigue properties mentioned above) are important to establish a database of properties for design and analysis of composite parts. However, continuum approaches provide little fundamental understanding of load transfer and failure mechanisms that occur at the micromechanics length scale where shear stress concentrations at the ends of a short fiber can induce fiber matrix debonding and localized matrix deformation as well as , tensile stress concentrations in adjacent fibers that lead to fiber failure. The role of fiber volume fraction, fiber length and gaps at fiber ends can also play an important role of damage evolution. In addition, micromechanics allows one to predict the effect of processing on material response and residual stress within the fiber and matrix. The state of residual stress at the micromechanics level also contribute to the evolution of damage due to static and fatigue loading.

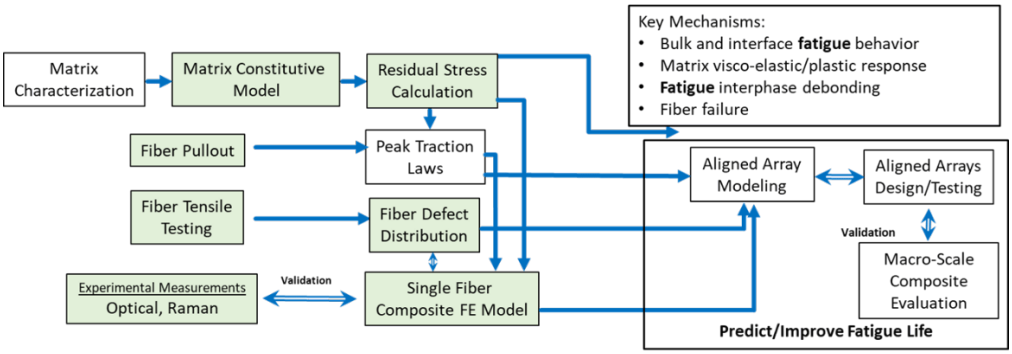

One of the processing challenges encountered this past year was the formation of wrinkles/waviness in the 3mm IM7/LM-PAEK unidirectional panels. This level of waviness was not seen in amorphous 3mm IM7/PEI panels studied last year. This level of waviness represents a critical microstructural defect that can dramatically degrade static properties and fatigue performance.

IM7/PEI
- No wrinkles present
- Full property translation

IM7/LM-PAEK
- Wrinkles present
- Inconsistant mechanical properties

The origin of the waviness was not known so we used our micromechanics methodology to visualize and monitor the evolution of fiber waviness as a function of cooling rates from the melt temperature for three polymers exhibiting a wide range of temperature dependent viscosity and degree of crystallinity (0 to 50%). By isolating the fiber waviness mechanisms at the filament level, it is possible to devise a processing method to minimize waviness and maximize a composite materials' mechanical performance (as proven out in the static and fatigue testing mentioned above).

Single fibers embedded in resin thin-films (between shimmed microscope slides) are pretensioned through melting/processing temperature of the resin, with a small (0.5 g) preload, to maintain a straight fiber at the start of the experiments. The pretension load is then removed at various temperatures along a cooling cycle (varying rates) to gain insight on how fiber waviness is affected by varying degrees of matrix/resin amorphous shrinkage. PP was chosen as a model resin because like LM-PAEK and PEKK it is semicrystalline and exhibits a large ΔT between processing and the onset of crystallization temperature. The experiment is conducted in a Mettler Hot-stage under a microscope that digitizes the fiber deformation under various cooling rates.

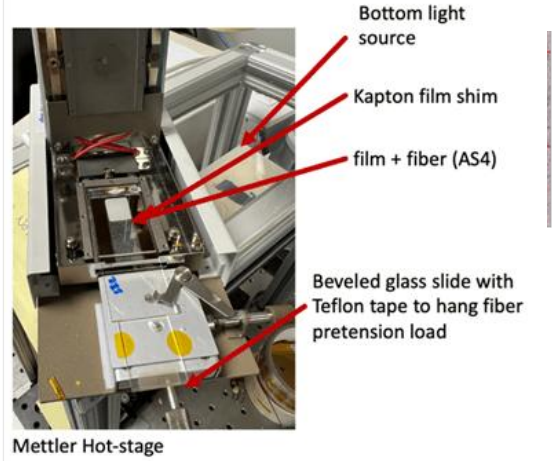

Mettler Hot-stage

The key observation was that waviness develops in the PP amorphous melt where the resin has low viscosity while undergoing thermal contraction. In this experiment the amplitude of the fiber waviness ceases at the onset of crystallization (130C) where the viscosity of the resin increases exponentially (starting at 20,000 P). Note that at the processing temperature of PEI of 330C the viscosity is also approximately 20,000 P, which is sufficient to resist fiber motion, and explains why PEI *TuFF* does not wrinkle

extensively. Conversely at the processing temperature of LM-PAEK (380C) the viscosity is much lower (10,000 P) resulting in the observed fiber waviness. The key to minimizing waviness in LM-PAEK is to reduce the process temperature to approximately 320C where the viscosity is comparable to PP and PEI polymers. Our novel visualization experiments on PP reveal that the evolution of fiber waviness is also dependent on the cooling rate of the process. High cooling rates (20C/min) are shown to reduce the amplitude of the fiber waviness by six-fold. Our planned activities for the coming year will focus on additional validation experiments and the development of a predictive model for process design to mitigate formation of fiber waviness.

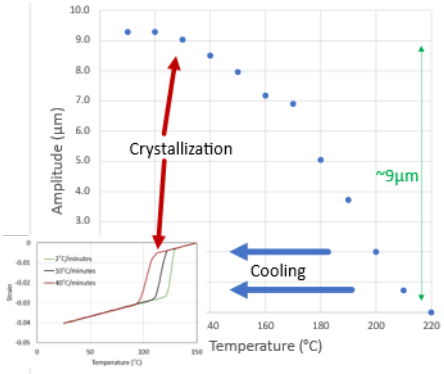

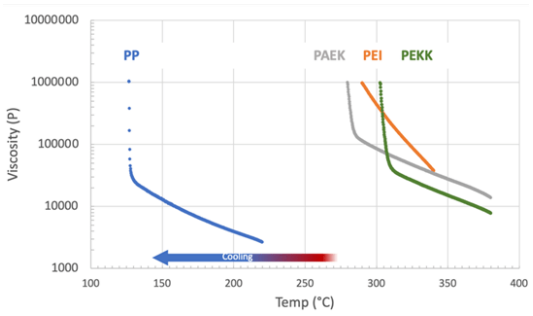

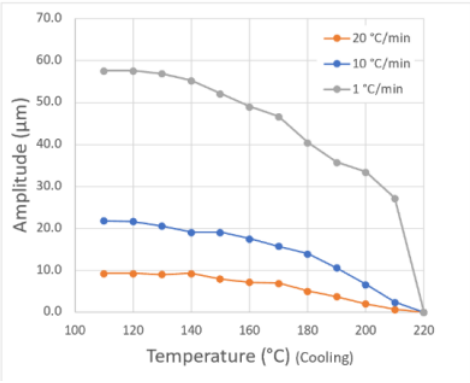

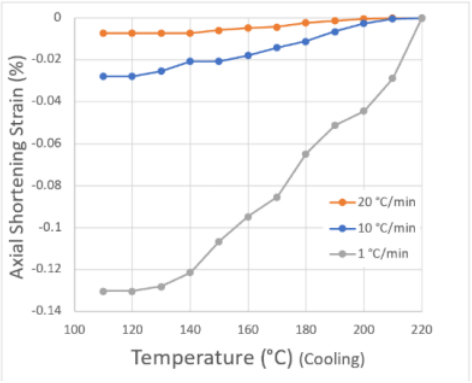

Although fiber waviness has been shown to cease at the onset of crystallization (or threshold viscosity), residual stress in the in the fiber and matrix develops during cooldown. The residual stress can be considered a pre-stress state that contributed to the onset of damage at the microstructural length scale. Frictional sliding at the interface can absorb significant amounts of energy during static and fatigue loading and is directly proportional to the radial compression associated with residual stress arising from the mismatch in CTE between the fiber and matrix.

A highlight from last year was the development of test method to measure axial compressive strain in a single carbon fiber due to processing using Raman Spectroscopy. A simplified model of residual stress was published using temperature dependent Young's modulus and thermal expansion in combination with the stress-free temperature defined at the end of crystallization that is very dependent on cooling rate (approach b in figure below). A computational

finite element (FE) model of thermal residual stress was developed for carbon fiber/thermoplastic composites and implemented via user material subroutine (UMAT) in ABAQUS. This year all simplifying assumptions were relaxes and the model for predicting residual stress included the complete non-isothermal crystallization kinetics from the amorphous melt to room temperature including the effects of crystallinity on temperature dependent resin modulus and resin shrinkage from both thermal and crystallinity (approach c). The key results show the importance of including the temperature dependent resin modulus versus traditional mechanics approach (approach a) and that the more comprehensive model validates the accuracy of the defining stress-free temperature as a function of cooling rate. This approach requires much less material characterization and is computationally much more efficient.

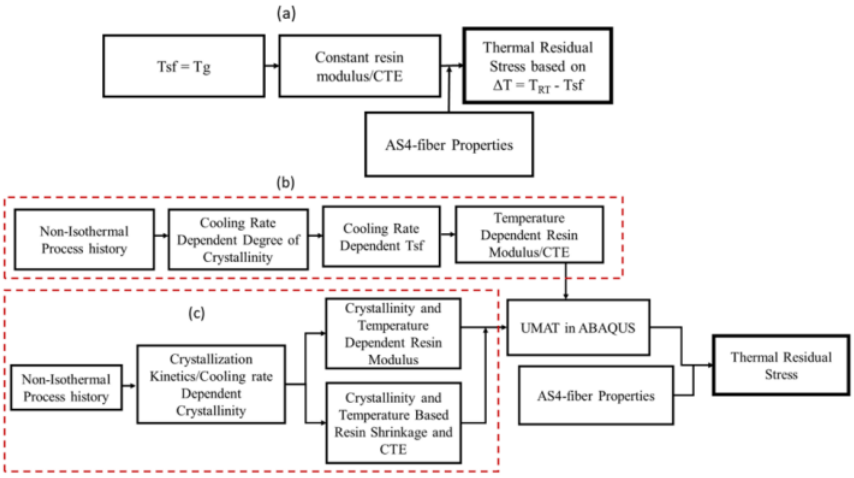

Flowchart for calculating thermal residual stress (Tg = Glass transition temperature and T_{RT} is room temperature).

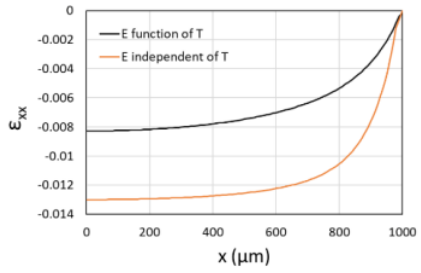

Neglecting temperature dependent resin modulus significantly overestimates the magnitude of residual axial strain by 50%

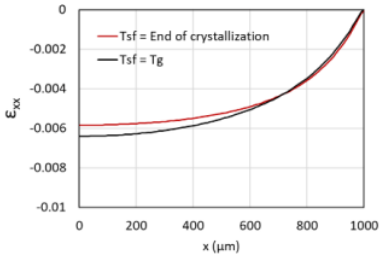

Validation of the Residual Stress Model Based on Cooling Rate Dependent Stress-free Temperature

Model validation of residual axial compressive strain in a single carbon fiber using Raman spectoscopy

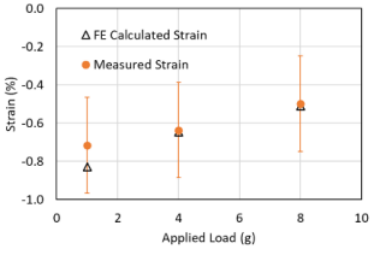

Insitu compression strain in carbon fiber is measured by Raman Spectroscopy to validate residual stress model

Highlights: Physics of Fiber Alignment

One of the key stages in the *TuFF* pilot facility is the alignment of short fibers into a preform used to make composite prepreg. Very little is understood about the physics of fiber alignment. A fundamental understanding of the alignment process is key to improving quality and throughput of the process and enabling the process to be optimized for all types of fiber. In the process, the short fibers are dispersed in a fluid at a high dilution ratio. During fluid extraction, the fibers decelerate with respect to the fluid velocity and are subjected to significant forces that provide the mechanism to align the fibers. The motivation for this study is to increase affordability of the alignment process by increasing throughput, minimize the probability of fiber breakage to retain mechanical properties and establish a predictive model to determine the limits of the process as a function of the fiber properties and aspect ratio. To achieve this goal a representation of the defects in a fiber are required to predict the location of potential fiber breaks and a physics-based model that describes the motion and deformation of a flexible elastic fiber in the fluid flow.

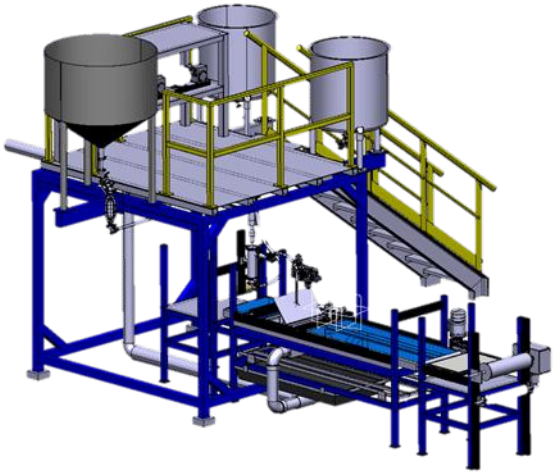

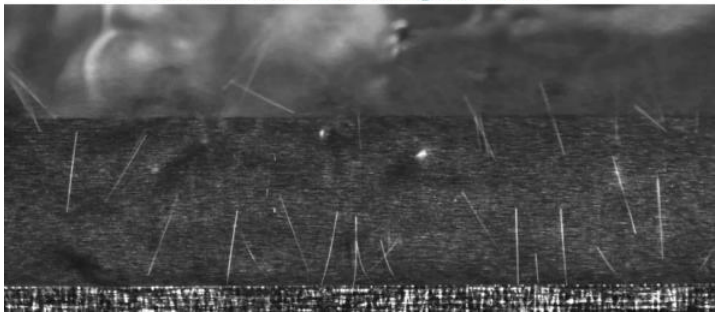

Fiber Landing Zone on the Spillway
5micron diameter, 3mm long IM7 Fibers

A novel single fiber bend test was developed to create a 3D map of surface defects on the fiber. In this test, a single fiber is placed between two Kapton films and bent around a small diameter wire and translated over 780mm. The wire radius uniquely defines the flexural strain applied to the fiber. The test is conducted in a confocal microscope and the location of the fiber break associated with this flexural strain is recorded. The test is repeated using the same samples and subjected to a smaller wire diameter that increases flexural strain and triggers additional

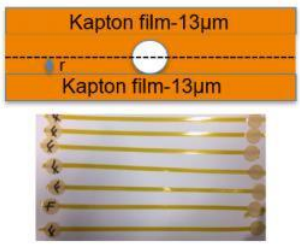

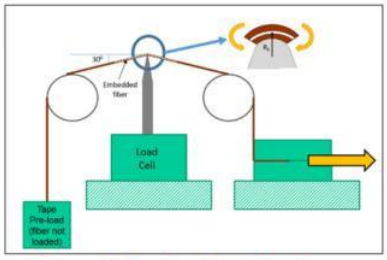

Schematic for bending test setup

The sample was pulled over the wire mounted on the tip of a razer blade. In this test method, the fiber is being exposed to flexural stress in continuous manner.

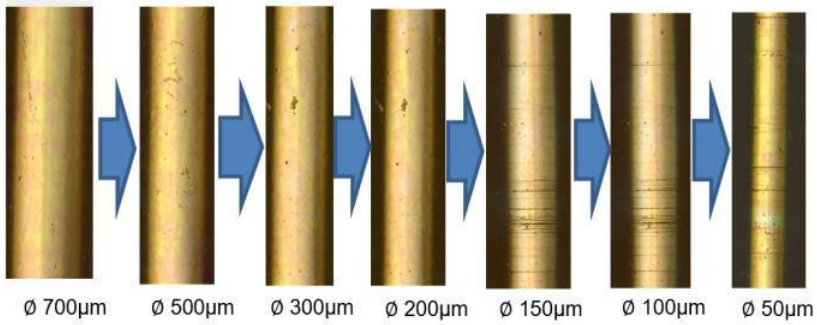

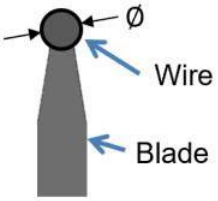

- Defect locations are captured from the images taken after each subsequent radius

defects (smaller). The location of these new defects is recorded.

Using this data, a quantitative 3D defect map is constructed relating defect spacing, defect size and flexural strain to failure/flexural strength. The experimental data is represented using a normal distribution and the assumption that the flexural strength is independent of the circumferential orientation of the fiber during the bending test. One of the independent validations of this new approach to map 3D defects onto single fibers is to use the defect map from the bending test to predict the cumulative probability of failure in a uniaxial tension test. Excellent correlation is found for the case of S2 glass fibers having a 2mm gage length.

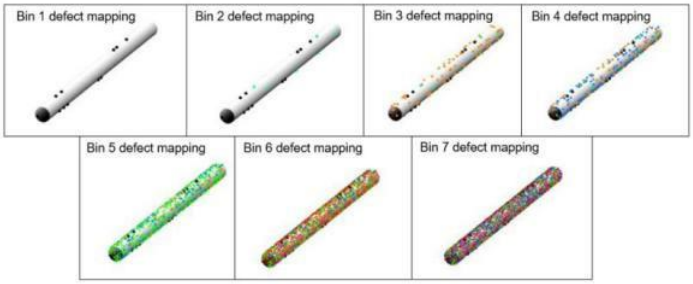

Schematic showing the bin-wise mapping of circumferential defects

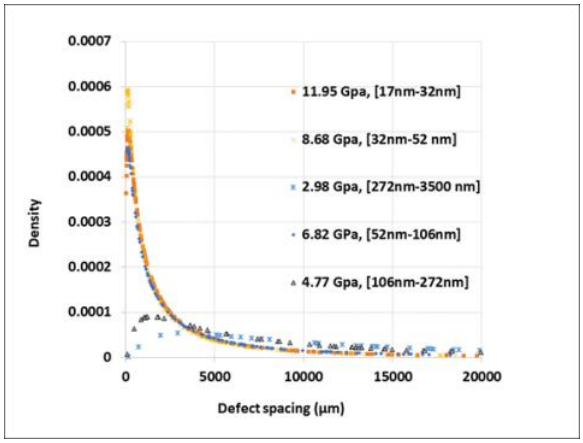

3D Defect Map Provides Excellent Correlation with Tension Test Data on S2 Glass Fiber with 2mm Gage Section

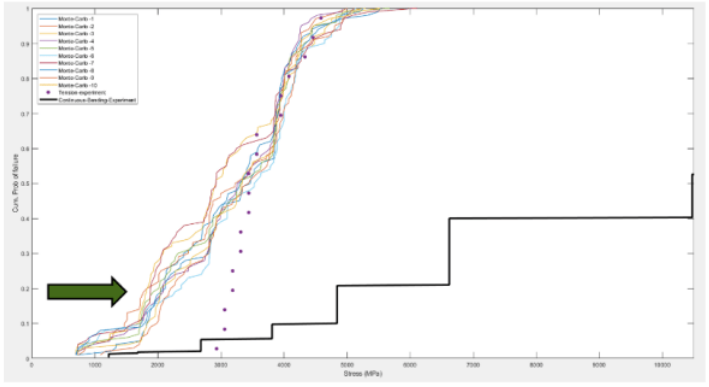

However, the current method also predicts the location along the gage section in which the fiber breakage will occur. This is essential information required for the prediction of length distribution after the fiber alignment process. Fiber breakage occurs at the defect location along the length of the fiber where the flow induced flexural strain that varies as a function of time is equal to the flexural strain to failure (or flexural strength) governed by the defect size.

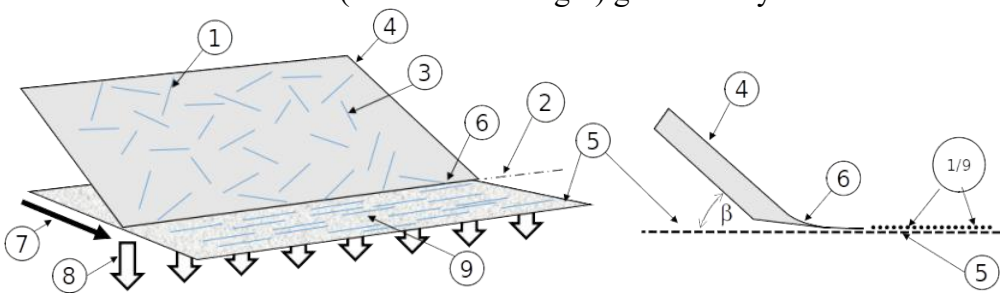

Schematics of TUFF fiber alignment process [1].(1) Reinforcement fiber in solution (2) Fiber landing zone (3) Water flow on spillway (4) Spillway (5) Conveyor belt (6) Shim (7) Belt Velocity (8) Water removal (9) Aligned fiber bed

A second highlight in this task is the extension of the governing equations to include higher Reynolds Number flow that enable drag forces along the fiber to be calculated more accurately. Recall our goal is to improve affordability of the alignment process by increasing throughput that requires higher fluid velocities.

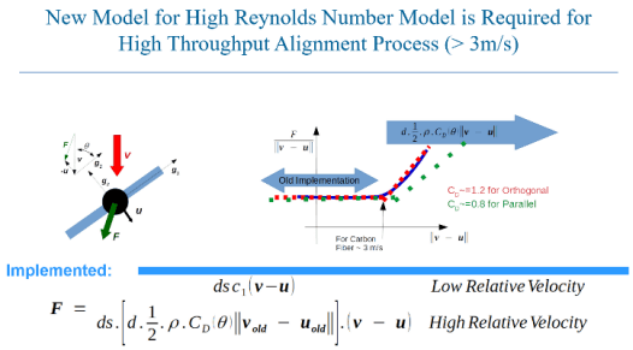

The governing equations are described and forces acting on the fiber are estimated. The numerical implementation of the model is described, and its numerical performance is evaluated. Several validation checks are performed to determine if the model is capturing the experimentally observed phenomena and if the estimated parameters provide reasonable quantitative agreement with experimental observations. At 1m/s flow rates, 3mm IM7 fibers are shown to rotate into the aligned position within 6-10ms depending on the initial approach angle of the fiber and the interaction of the fiber end with the belt (pinned or simply supported). The results clearly show that the location of maximum bending moment/flexural strain varies as a function of time and location along the fiber length and is very dependent on the fluid velocity. This is essential information for the prediction of the location of fiber breaks when combined with the 3D defect map as a function of fluid velocity.

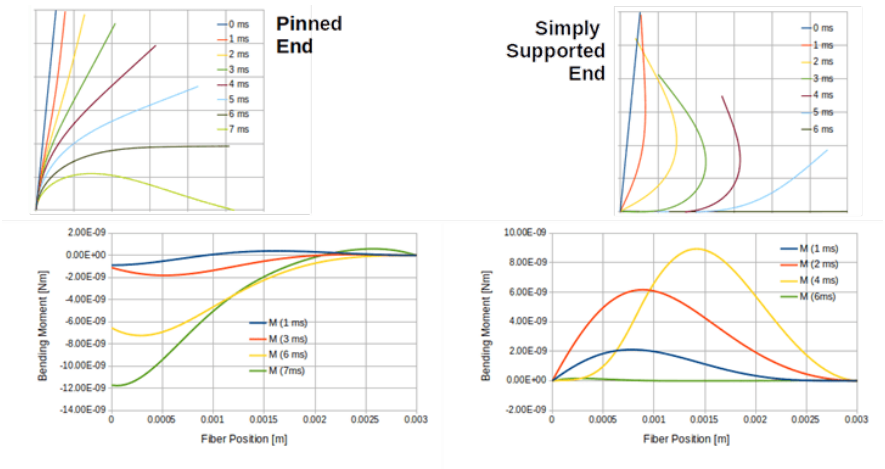

Deformation progress and the development of bending moment for fiber arriving at 85 degrees, either pinned or simply supported.

The two models have been integrated to study the effects of fluid velocity on the number of breaks and the final aspect ratio distribution. The key results confirm that the current standard operating conditions (1m/s) do not break fibers. Of greater importance, the model shows that the throughput can be increased by a factor of 10-20 fold before significant fiber breakage will occur. Since fiber alignment is one of the cost drivers for the overall *TuFF* process, these results show significant promise for improving affordability without degrading structural properties.

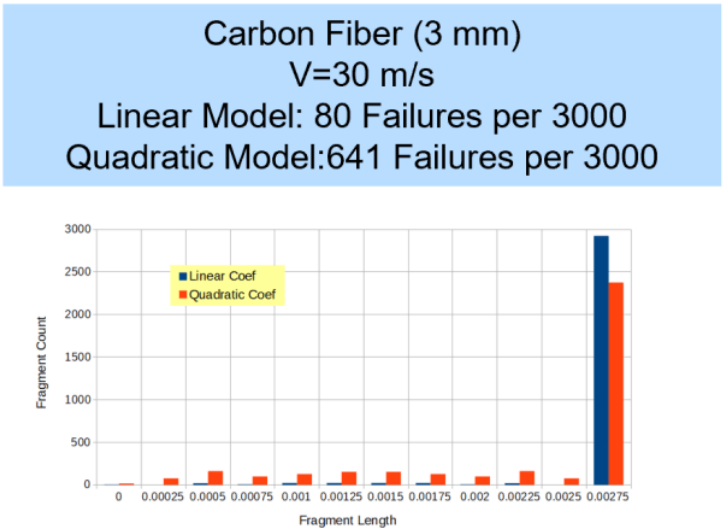

Highlights: Micromechanics of Anisotropic Viscosity and Forming of TuFF Composites

The primary objective this task is to develop simulation capabilities to predict thermoplastic *TuFF* composite material properties after forming. In order to develop a blank forming process simulation, fundamental material properties related for forming aligned discontinuous fiber *TuFF* composites need to be experimentally determined. These properties fall into two categories: constitutive material laws governing the mechanics of deformation of a (molten thermoplastic containing high volume fraction of aligned short fibers) *TuFF* blank and the

forming limits of the material (i.e., strain limits that degrade properties after part forming). Similar to metal forming, the material forming limits (ultimate strain) are anticipated to be independent of the material. In a forming simulation the constitutive laws of deformation will govern the relationship between stress, strain, strain rate, and temperature to predict key properties of the formed part (formed strain, thickness, and fiber orientation). In its simplest form, a *TuFF* material forming limit curve would be implemented as formed material strain limit, which cannot be exceeded. A forming limit may also be related to material stress through temperature and strain rate.

The current state of the art for the constitutive laws of deformation are based on the theoretical framework of a single fiber unit cell to determine the anisotropic viscosity tensor. The theory was first applied to aligned discontinuous fiber composites (for modeling forming of stretch broken carbon fiber) by linear approximation of the shear between fibers[1,2]. These models are quite useful because they include all viscosity tensor components. This model framework was improved by resolving the unit cell problem with respect to a fluid suspension[3]. In recent year, the model has been more rigorously extended to non-Newtonian polymer melts (albeit low concentration fiber suspensions)[4]. Ultimately, experimental data of highly concentrated aligned discontinuous fiber composites (for SBCF samples) was under predicted by the extensional viscosity model[5]. The unit cell model is an extremely useful framework in that the effect of the microstructure properties can be deconvoluted from the polymer rheological properties and does not use any fitting parameters. In this year's task effort, the unit cell rheological model has applied the work of Creasy & Advani, 1996, (with a correction) and extended the model to shear thinning and Carreau-Yasuda rheological models. The models enable the actual shear strain and shear strain rates (and relaxation times) to be estimated at the microstructural length scale as a function of fiber volume fraction and aspect ratio. A magnification factor shows that the deformation rates within the microstructure are 3-5 orders of magnitude higher than applied to the continuum. Future work will focus on improving the correlation between the model predictions of temperature dependent extensional viscosity with experimental measurements.

Forming limits of aligned discontinuous fiber composites has no directly applicable framework in the literature. Previous work on isotropic metals[6] and isotropic composites[7], do not account for differences in strain limits by material direction which arise from the fundamental difference in failure modes relative to the longitudinal and transverse fiber directions.

Technical Highlights in Experimental Characterization for Developing Constitutive Model

Progress towards developing the constitutive laws of deformation has focused on defining the the extentional viscosity ($\eta_L \approx \sigma_L/\dot{\varepsilon}_L$) of *TuFF*/PEI (processing challenges of making wrinkle-free *TuFF*/LM-PAEK were only recently overcome as noted above) in terms of the properties of the constituent materials. Characterization with PEI as the matrix polymer has continued because it serves as an excellent surrogate material for this purpose. Since PEI is amorphous, the range of temperatures which can be characterized (with respect to the glass transition temperature) is much

[1] R. B. Pipes, J. W. Hearle, A. J. Beaussart, A. M. Sastry, R. K. Okine, A Constitutive Relation for the Viscous Flow of an Oriented Fiber Assembly, Journal of Composite Materials 25 (9) (1991) 1204-1217.
[2] R. B. Pipes, D. W. Coffin, S. F. Shuler, P. Simacek, Non-Newtonian Constitutive Relationships for Hyperconcentrated Fiber Suspensions, Journal of Composite Materials 28 (4) (1994) 343-351.
[3] T. S. Creasy, S. G. Advani, A model long-discontinuous-fiber filled thermoplastic melt in extensional flow, J. Non-Newtonian Fluid Mech 73 (1997) 261-278.
[4] J. Ferec, E. Bertevas, B. C. Khoo, G. Ausias, N. Phan-Thien, The effect of shear-thinning behaviour on rod orientation in filled fluids, Journal of Fluid Mechanics 798 (2016) 350-370.
[5] T. S. Creasy, S. G. Advani, R. K. Okine, Transient rheological behavior of a long discontinuous fiber-melt system, Journal of Rheology 40 (4) (1996) 497-519.
[6] ASTM E2218 - Standard Test Method for Determining Forming Limit Curves
[7] Dessenberger, R. B., & Tucker, C. L. (1998). Forming limit measurements for random-fiber mats. Polymer Composites, 19(4), 370–376.

higher than for a semicrystalline polymer. The methodology for characterizing the extensional viscosity of *TuFF*/PEI is the same as documented in the previous year's report. The objective is to explain *TuFF* extensional viscosity in terms of the rheological properties of the polymer and the microstructural properties of the aligned discontinuous fiber bed. If a suitable micromechanics model can be formulated and validated, a general approach can be designed to predict and tune the *TuFF* extensional viscosity from the constituent inputs. A validated constiutive model and material database is an essential input to our overall modeling approach for *TuFF* parts.

The viscosity of Ultem 1000 was characterized with oscillatory rheology on TA Instruments DHR2. In isothermal conditions a frequency sweep was used to observe strain rate depencance. The test was repeated at a range of temperatures (250-350C) above the glass transition temperature (Tg=217C), shown in a), and then assembled into a master curve at the reference temperature of 330C using the time-temperature-superposition (TTS) prinicple, shown in b).

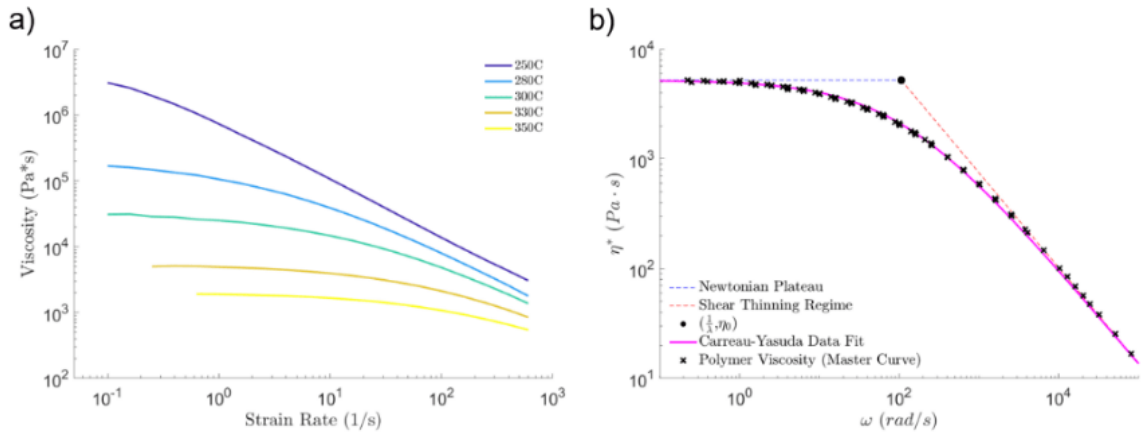

Viscosity of Ultem 1000 PEI

The shift factor will shift both the newtownian plateau and the relaxation time.

$$a_T = \frac{\eta_0(T)}{\eta_0(T_0)} = \frac{\lambda(T_0)}{\lambda(T)} = \exp\left[\frac{E_a}{R}\left(\frac{1}{T} - \frac{1}{T_0}\right)\right]$$

Table 1 shows the shift factors which allow a) to shift to b).

Table 1. Shift factors

T (°C)	α_T	β_T
250	3190	1.15
280	40.5	1.09
300	6.25	1.05
330 (T_0)	1	1
350	0.352	0.968

The Carreau-Yasuda model was fit to the data using the parameters in Table 2.

$$\eta = \eta_0(1 + (\lambda_0\dot{\gamma})^{\mathrm{a}})^{\frac{n-1}{\mathrm{a}}}$$

Table 2. Carreau-Yasuda model parameters for Ultem 1000 PEI.

η_0 (Pa*s)	λ_0 (s)	n	a
5200	0.0094	0.13	0.65

The micromechanics model assumes a uniform array of aligned and staggered fibers. The spacing of fibers is defined by the fiber volume fraction. The figure below (d) shows a cross-section of *TuFF*/PEI with local fiber volume fraction overlayed. Local fiber volume fraction is a distribution (58±8%), and the effect of this source of variablity on the extensional viscosity is not understood at present. The extensional viscosity of the *TuFF* composite is governed by the shear stress and rate of the polymer between fibers.

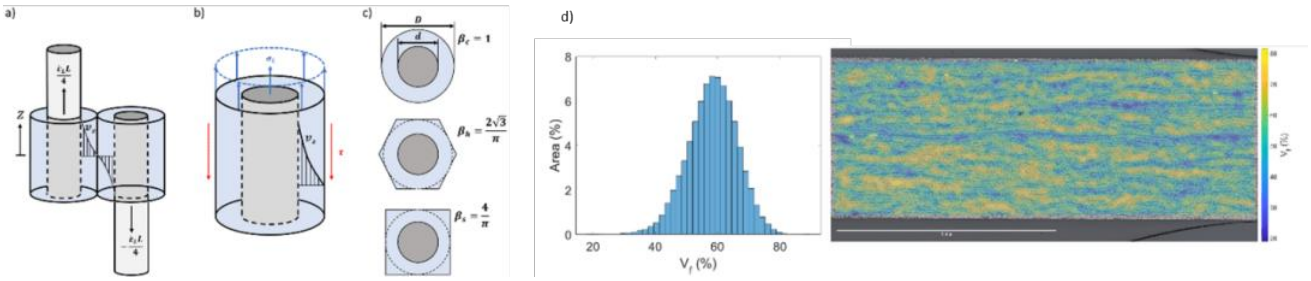

Micromechanics unit cell model. (d) *TuFF*/PEI [0]6 cross-section and measured local fiber volume fraction from image analysis.

Starting from the govering equation $\nabla \cdot \sigma = 0$, the viscosity can be solved exactly for cases where the polymer is Newtonian ($\eta = \eta_0$)

$$\eta_L = -\eta_0 \frac{V_f}{2\ln\sqrt{\beta V_f}}\left(\frac{L}{d}\right)^2$$

Or shear thinning ($\eta = K\dot{\gamma}^{n-1}$)

$$\eta_L = K\left(\frac{1-n}{2n}\right)^n \frac{V_f}{\left(1-(\beta V_f)^{\frac{n+1}{2}}\right)^n}\left(\frac{L}{d}\right)^{n+1} \dot{\varepsilon}_L^{n-1}$$

The two above equations intersect at the relaxation time. With the relaxation time being the inverse of a particular strain rate, the equation below also represents the shear magnification—the shear rate in the polymer relative to the composite extensional strain rate.

$$\lambda_L = \lambda_0\left[\left(\frac{1-n}{2n}\right)^n \frac{2\ln\sqrt{\beta V_f}}{\left(1-(\beta V_f)^{\frac{n+1}{2}}\right)^n}\right]^{\frac{1}{n-1}}\left(\frac{L}{d}\right)$$

Table 3. Average and standard deviation of composite microstructre values

V_f	L/d	β
0.58 ± 0.08	630 ± 100	$2\sqrt{3}/\pi \leq \beta \leq 4/\pi$

The extentional viscosity for *TuFF*/PEI was measured for strain rates between 1e-4 and 1e-2 s-1 at temperatures of 300, 330, and 350C. The TTS shift factors for the polymer were applied to the extensional viscosity data to show that the data can collapse to a master curve at the reference temperature (330C). This result is expected because the polymer viscosity can be factored out of the extensional viscosity model above.

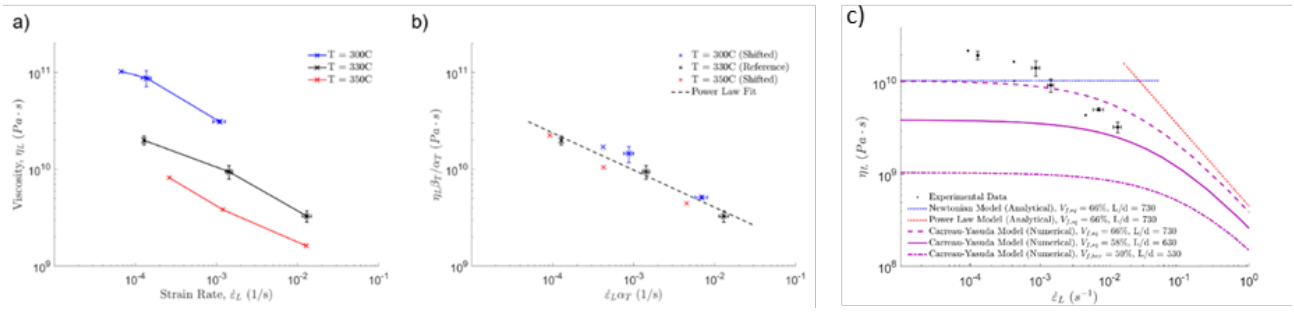

(a) *TuFF*/PEI [0]2 extensional viscosity. (b) TTS shift factors from Table 1 are applied directly to the extensional viscosity data. (c) The micromechanics model with upper and lower bounds (from Table 3) do not capture the measure *TuFF* extensional viscosity.

The micromechanics model was solved numerically for a Carraeu-Yasua polymer to determine the viscosity transition between newtonian and shear thinning. The figure shows the micromechanics model appled for average material values (from Tables 2 and 3), as well as 1 standard deviation above and below. The result shows that including the standard devation does not properly bound the measure composite extensional viscosity results. Future work will investigate new mechanisms which contribute to the extensional viscosity response.

Forming Limits of Aligned Discontinuous Fiber Composite Laminates

Investigation of material forming limits has looked at the evolution of material microstructure as well as development of an overall framework to define how to quantify forming limits into a process design diagram, which is applicable to an anisotropic composite *TuFF* blank.

It was shown previously that thermoplastic *TuFF* composite will deconsolidate similarly to a typical continuous fiber thermoplastic composite when heated to process temperatures without any consolidation pressure. The extent of deconsolidation (thickness increase) is higher due to the slight differences in fiber alignment (95% of the fibers in *TuFF* are aligned within +-5° compared to +-3° in continuous fiber composites). *TuFF* is typically consolidated with >200psi of pressure. When reheated without pressure, the microstructure will deconsolidate to >50% (shown below) and a corresponding porosity of 32%. This is not problematic by itself because this porosity can be reconsolidated to produce the same quality laminate. The question raised when looking at microstructure evolution is how does uniformity change during deformation and how will this affect the forming limits of the material.

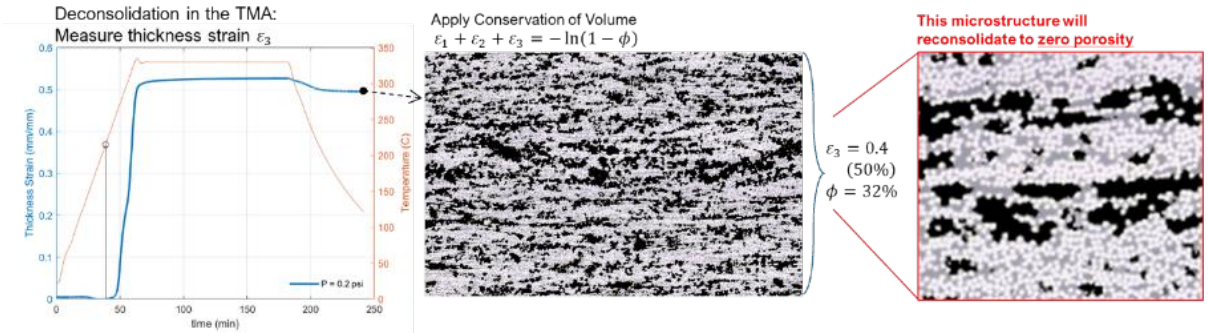

TuFF/PEI [0]6 deconsolidation in a TMA.

To determine the evolution of microstructure uniformity, series of samples were prepared (*TuFF*/PEI [0]6) and stretch to lengths up to 65% elongation, (shown below). At the test conditions, no tearing of the material was observed for any of the samples, nor did the composite stress strain curve have any indication of failure onset.

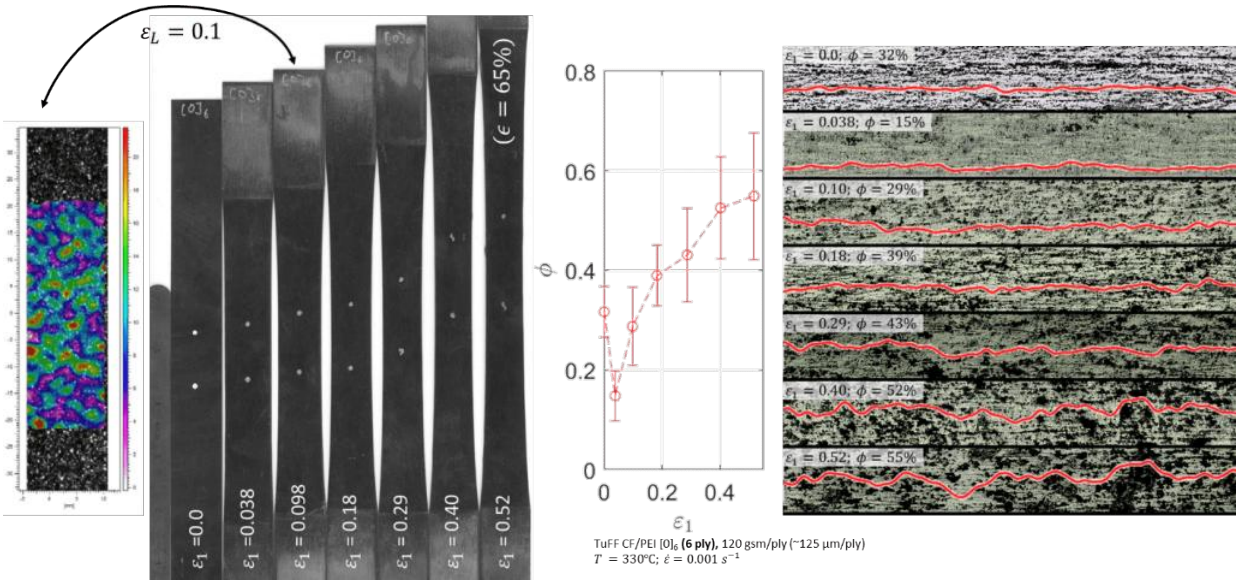

TuFF/PEI [0]6 samples were stretched in uniaxial extension to investigate the evolution of microstructure. Micrographs show level and variability of porosity as applied strain increases. Porosity level and variability with applied (true) strain.

Samples microstructure was investigated with x-ray micro-CT of the full gage section, as well as with high resolution optical micrographs of cross-sections of the full gage width. The figure shows image processed micrographs which include a moving average of through-thickness porosity. The graph summarizing the micrographs shows that overall porosity increases as well as porosity variability during forming. The variability is the factor which may have an impact on the ability to reconsolidate the sample after forming.

The framework for defining a forming limit diagram for anisotropic aligned discontinuous fiber composites with respect to material direction is shown below. Since the failure mode changes by material direction, the strain capacity will also change by direction. The failure strain in a formed part must be determined with respect to the biaxial strain of each ply in a laminate structure.

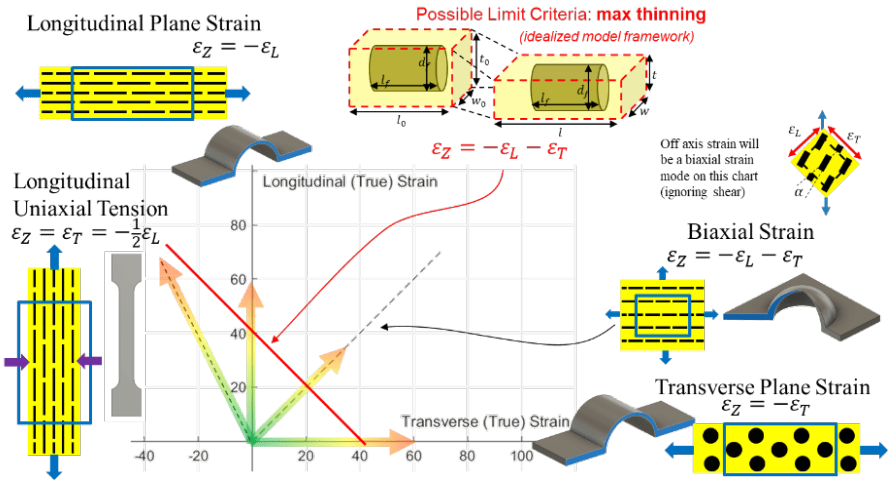

Proposed aligned discontinuous fiber forming limit diagram framework.

In order to evaluate material quality according to this diagram, parts were formed which induced varying strain levels and strain modes. Blanks were formed into cylindrical (bead stiffener) molds of 3 depths. The process was isothermal, with the gas pressure increasing at a rate of 5psi/min up to 100psi, and then the pressure was increased to 300psi for final consolidation. Blanks were patterned with regular spaced dots in order to measure the biaxial strain.

TuFF/PEI $[0/90]_{2s}$ blanks were prepared for the set of trials. The figure below outlines the steps of the experimental procedure. The cross-ply laminate sequence ensured that both longitudinal and transverse ply strain were induced in each part. All blanks were c-scanned to observe the initial consolidation quality. Blanks were also 3D scanned to observe the initial thickness uniformity. After forming, blanks were 3D scanned again. The dot pattern was measured using surface profile distances with the CMM features of the 3D scanner. Thickness was also assessed with the 3D scanner after forming. This process allows the full 3D strain tensor to be measured. After completing all strain measurements, samples were cross sectioned to determine the consolidated composite quality. Cross-sections in orthogonal directions were used to determine the quality of plies which experienced longitudinal strain (0-degree plies) and transverse strain (90-degree plies).

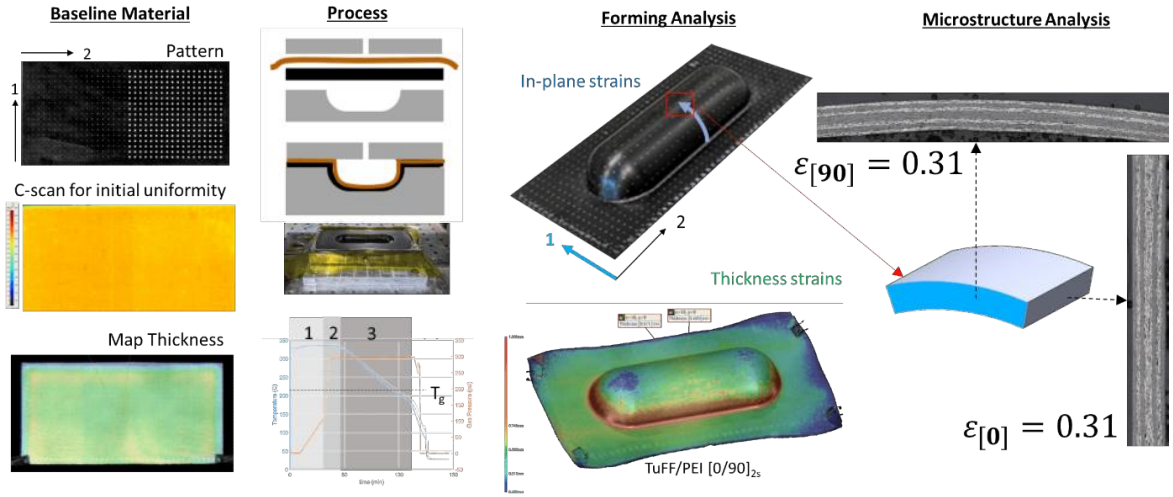

Material quality evaluation, measurement of the full strain tensor and post forming material quality assessment from material cross-sections.

From the 3 mold depths used to form the sample set, the measured strain in each sample (in the hoop direction) was 0.075, 0.21, and 0.31 true strain. The figure below shows the material cross-sections arranged for each sample, as well as a cross-section of the blank for reference. By aligning and scaling each micrograph, it becomes visually apparent that the entire laminate is thinning as it elongates. Furthermore, each ply appears to thin uniformly with respect to the laminate. No splitting or non-uniform ply structure was observed in this sample set.

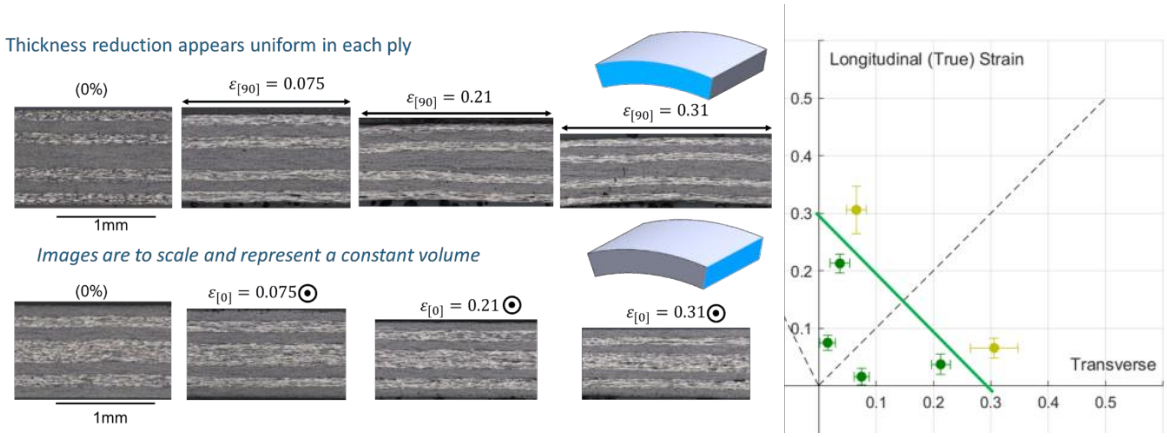

Orthogonal material cross-sections (*TuFF*/PEI [0/90]2s) of formed samples with increasing levels of (true) strain. Preliminary *TuFF*/PEI forming limit diagram. Some porosity is observed in samples with 0.3 (true) strain so the quality is labeled as marginal until more testing can be completed. The results are plotted on a forming limit diagram according to the level of strain and strain mode and quality of the material cross-section.

As an example, this figure also shows the results assembled into a preliminary forming limit diagram (as proposed above) based on porosity. Some porosity is observed in the highest strained sample; therefore, this sample will be marked as marginal quality until a robust quality metric can be defined. Porosity is observed in both 0- and 90-degree plies so material direction limits cannot be clearly distinguished with this sample size. A preliminary forming limit is simply drawn diagonally between 0.3 plane strain modes. Future work will explore both biaxial strain modes and higher strain levels with this methodology. Other considerations for the forming limit will be based on allowable thinning and stiffness and strength of post-formed samples that would be very useful for process, tooling, and part design.

Forming Software Evaluation

This task aims at identifying commercial software platform to simulate the forming process of the *TuFF* material. This can be accomplished by the use and necessary modification of available software (preferably) or developing a new implementation through user development subroutines.

In existing package, the modeling entails providing material description for a single ply of the *TuFF* material and utilize the other package features as they are. So far, we have evaluated several packages to determine their suitability for modeling of *TuFF* forming.

To accommodate *TuFF* forming in existing package, the requirements were formulated as

- Software must handle proper material model. This means viscous or visco-elastic plies with high anisotropy (ratio of 10,000 between longitudinal and transverse viscosity). This requires support for the proper model (or user material to implement it) but also proper numerical stability.

- Software can handle proper ply to ply and ply to tool interactions. Currently, our knowledge of these is limited.
- The software can handle applicable forming processes. This includes proper tooling sets, like match metal or diaphragm and simulation of necessary heating mechanisms and temperature development.
- The software provides the necessary outputs like layer deformation, fiber orientation, thinning and thickening and ply shape design.
- We will need to cooperate with the software vendor to implement and correct whatever is needed.

This past year we have been assessing two packages – Aniform and Altair's Hyperform – in some detail. Hyperform is metal based with development of composite functionality under current development. Aniform specialized in composite forming but is currently limited to isothermal process (non-isothermal forming processes cannot be considered at the present time). The comparison is provided in the table below.

Comparison of forming packages.

In the past year, a collaborative project with Altair was undertaken to assess the capability of Hyperform's existing material models to model the stretchability of *TuFF*. In addition, our micromechanics model for extensional viscosity discussed above was also implemented by Altair in as a user material subroutine. Altair concluded that the current platform was not capable of modeling *TuFF* as their core solver is based on structural mechanics (force-displacement) were

	Aniform	Hyperform
Proper Material Model	In Theory Only	No but User Material System
Proper Ply Interactions	Simplified but OK	Simplified but OK
Model Can Handle Applicable Processes	Process Yes No Temperature Solver and Dependence	Processes Yes Temperature Yes
Model Provides Proper Outputs	Layer and Fiber Orientation Tracked, Thinning/Thickening ...	Layer and Fiber Orientation Tracked, Thinning/Thickening ...
Company Willingness to Cooperate	Yes but Very Limited Resources	Yes

constitutive laws are based on non-linear stress strain response having strain rate dependent elastic and nonlinear plastic behavior. This approach is used successfully to describe forming of materials near the softening temperature (e.g., Tg, melt). *TuFF* constitutive response is stress vs strain rate

and has no elastic behavior (removal of strain rate results in a rapid relaxation to zero stress) as the process temperature is well above the melt temperature of the thermoplastic matrix. *TuFF* is also highly anisotropic with transverse/shear viscosities being 10^5-10^6 lower than the extensional viscosity in the fiber direction. Various attempts over a period of 3 months were made to approximate this behavior on single element and small models but all the results were numerically unstable. In parallel, our group has collaborated with the developers of Aniform to assess their code for implementation of *TuFF* constitutive behavior. Preliminary results are promising, and UD has purchased a license to continue this study. Since this is a very challenging but important topic, we also plan to evaluate ANSYS software (LsDyna) and Abaqus for forming capabilities.

Highlights: Process Development

The second year focused on the development of the forming work cell at UD-CCM and the collaborations on part selection and process development with our industrial partners (Joby, Spirit Aerospace and ATC). Monthly meetings are held with the industrial partners and in-person visits have been held at all three companies. Joby has provided CAD/CAE drawing packages for a door component on their UAM vehicle, fabricated a tool and delivered the tool this summer. Joby engineer is visiting UD-CCM to participate in process development.

Forming Work cell Developments

During the past year, process development has focused on thermoforming trials using surrogate blanks to prove out the work cell comprised of a pick-and place ABB robot, a 120 kW IR oven for rapid heating of *TuFF* blanks and a 1000-ton press for forming. The IR oven control software has been updated to include multiple pyrometer temperature setpoint triggers for blank extraction from the oven to the press to prevent part temperature overshoot. Experiments have been conducted to optimize IR oven conditions to ensure blank temperature uniformity. The press control software has been integrated with the robot to minimize process cycle times and ensure successful part handoff. Efforts have also focused on modeling heating rates and uniformity of temperature achievable in the oven and the speed/cooling rates for transport of the heated blanks by the ABB robot to the forming press. Radiation simulations of this transient process have been developed for the IR oven and thermal models have been developed for the forming process using surrogate materials for simple die geometries and a waffle mold to predict contact-cooling rates in the mold.

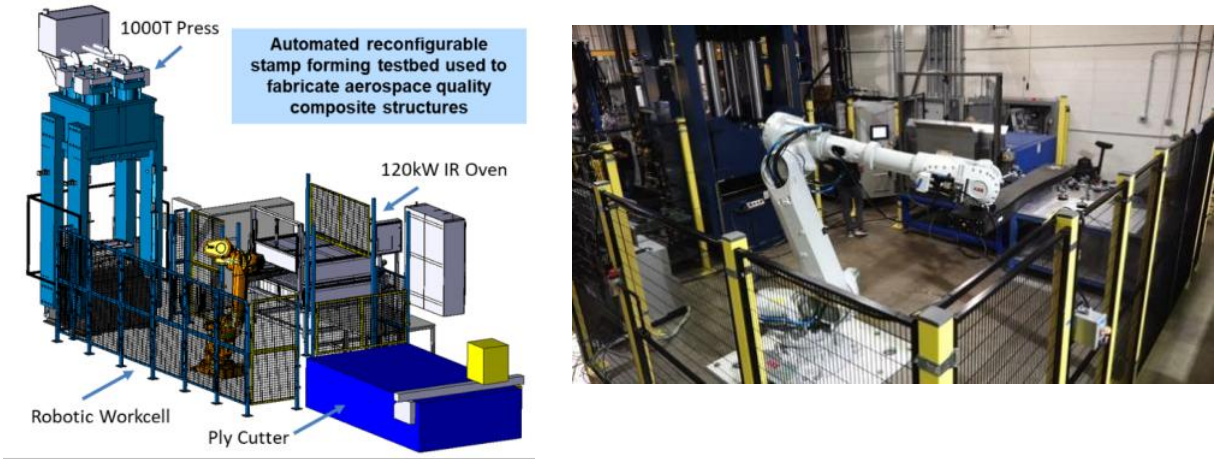

UD-CCM High Speed Thermoforming Workcell (2019 ONR DURIP)

Polycarbonate panels are used to prove out the forming work cell at rate with two-minute process cycles demonstrated. Polycarbonate is a well characterized material in terms of non-isothermal viscosity and as an isotropic polymer is possible to simulate the forming process. Forming repeatability and consistency has been demonstrated for this process using a waffle mold as shown below (this is the same mold used to successfully demonstrate stretch forming of *TuFF* under isothermal conditions).

In parallel, forming simulations for this geometry using polycarbonate have been developed in Abaqus to predict deformation and temperature profiles as contact occurs over time between the blank and mold walls. This model considers the blank as a 3D volume to capture through thickness thermal gradients and will be extended to model *TuFF* behavior once material models have been established and forming code selected. Experiments are currently ongoing to validate model predictions by fusion bonding embedded thermocouples with strain relief at key contact locations within surrogate polycarbonate panels. Experiments are also ongoing with partial forming to establish panel strains and thickness distribution using a Keyence VL-500 system as a function of crosshead location and tool temperature. These experiments will aid in developing DOE protocols for waffle forming *TuFF* panels in the coming year once material models are established.

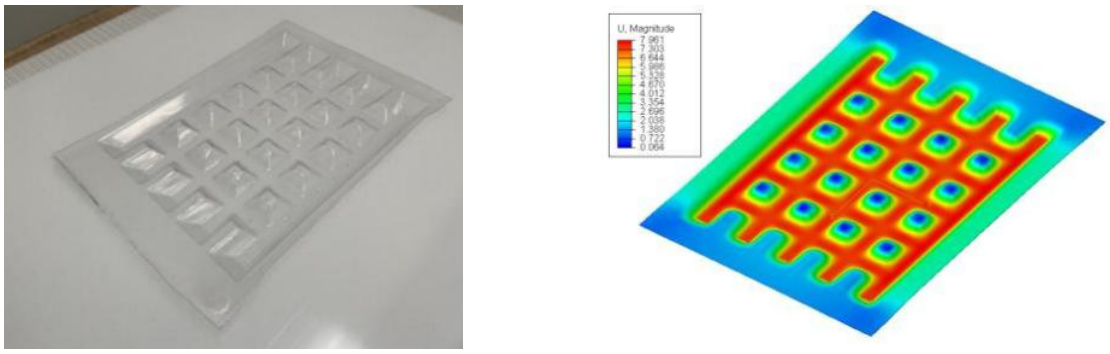

Thermoformed polycarbonate and associated FE forming simulation

In addition to waffle forming, die forming simulations have also been developed to accurately capture temperature gradients within the deformed part as well as optimize FE design for larger scale models. These simulations are used to support model experiments for a die forming work cell that will also be operational in the coming year (2022 ONR DURIP). This cell accommodates real time measurements of surface strain and temperature using a Trillion Digital Image Correlation System and our IR camera system. This model includes contact pressure driven conductance that determines part heat flow into the tool walls that will be validated using embedded thermocouples in thermoformed panels. It can also be used to access part thinning as a function of temperature differential between incoming blank and tool surface. These highly instrumented forming trials will enable validation of the simulations throughout the transient forming process.

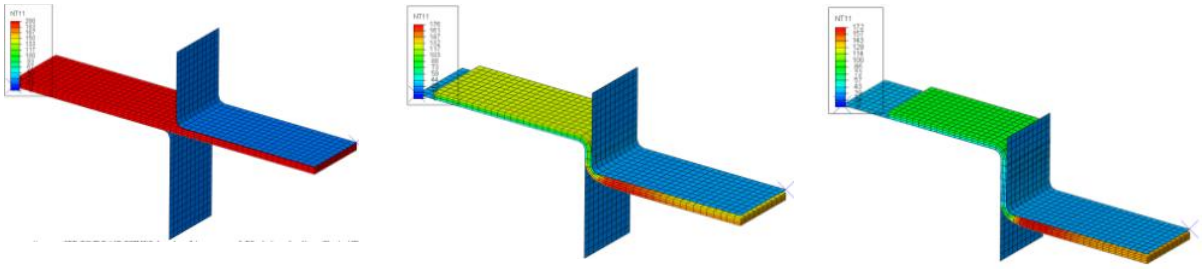

Transient thermal model for punch die forming, predicting heat flow from part into mold walls as a function of contact pressure distribution.

A heat transfer model for the IR oven have been developed in ANSYS to predict panel temperatures exposed to radiation emitted from a series of heater filaments above and below the composite blank. This model, shown below, also includes stationary hot air convection to the panel, and is used to optimize energy distribution to the part based on size, thickness, and geometry. The half symmetry model considers the coils at a specific temperature and scaled area, based on the coil surface area and volume. The oven itself has independent heater control in three zones from rear to front (HZ1,HZ2,HZ3) with a pyrometer controlling each zone. The infrared images of a large 4'x3' panel heated independently with each zone (a-c) exhibits large in plane temperature gradients. The image of the panel heated with optimized energy distribution has uniform heating (d). Heater zone interactions based on view factor requires iterative steps to determine the best heat distribution to the part surface. The radiation model predicts optimal energy input distribution in each zone based on these overlapping view factors between heater coils and composite panel without the need for iterative trial and error experiments. It can also be used to aid in design of local radiation shielding that can be used to tailor energy distribution for parts of varying thickness. This prevents overheating of thin sections while allowing the centerline temperatures of thick regions to reach the prescribed forming temperature. The models ultimately aid in providing optimal process cycles that rapidly heat composite blanks uniformly without overshoot and can provide ideal pyrometer target locations as a process monitoring control.

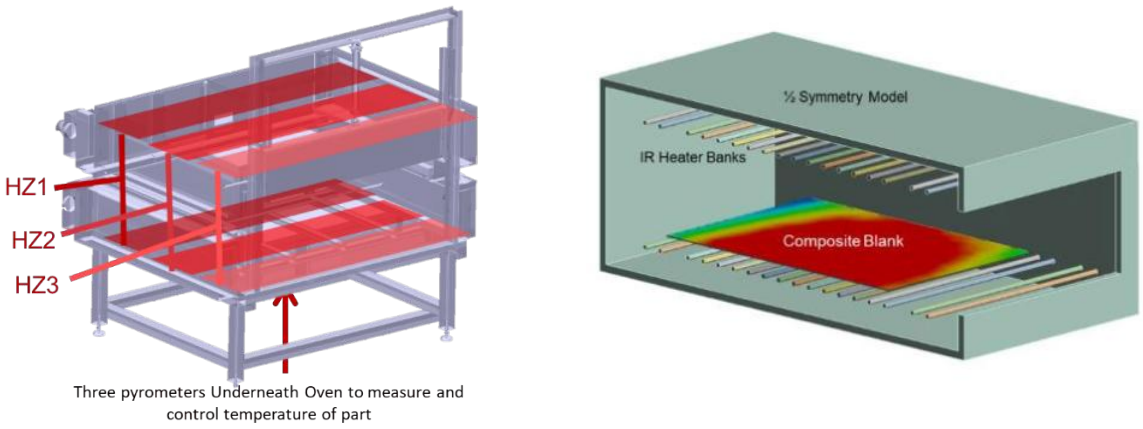

Half Symmetric FE Model of IR Oven captures radiation view factor to panel surface and air convection heat distribution within the composite panel

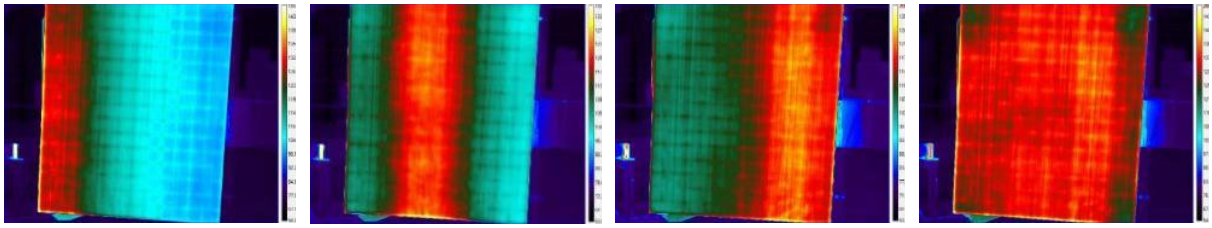

(a) *(b)* *(c)* *(d)*

Infrared images: (a) HZ1 only, (b) HZ2 only, (c) HZ3 only heating and (d) optimized zone heating for a large 4'x3' composite panel (corners cooled by vacuum cups post retrivel)

To summarize, the forming cell is currently being used to establish guidelines for assessing transient thermal conditions in the IR oven and forming mold using surrogate panels. Embedded thermocouples fusion bonded within neat polymer panels will capture internal part temperatures during heating, transport and forming. In addition, partial forming studies will be used to access strain and thickness profile distributions during forming. These studies will establish metrics for accessing *TuFF* panel forming by understanding the challenges of measuring part temperature and thickness distribution. Results from these experimental studies will be presented at the upcoming ULI review.

TuFF Part Demonstrations with Industry Partners

In this effort, UD-CCM is collaborating with Spirit AeroSystems and Joby Aviation to identify complex geometry composite parts that are candidates for *TuFF* forming demonstrations. Spirit has identified the thrust reverser cascade as a demonstration component, and Joby has identified a door frame on their air vehicle due to its complex geometry and curvatures. Both parts are shown below. Collaborations are on-going with both Spirit and Joby in the form of weekly/bi-weekly calls for technical discussions and progress updates, as well as site visits.

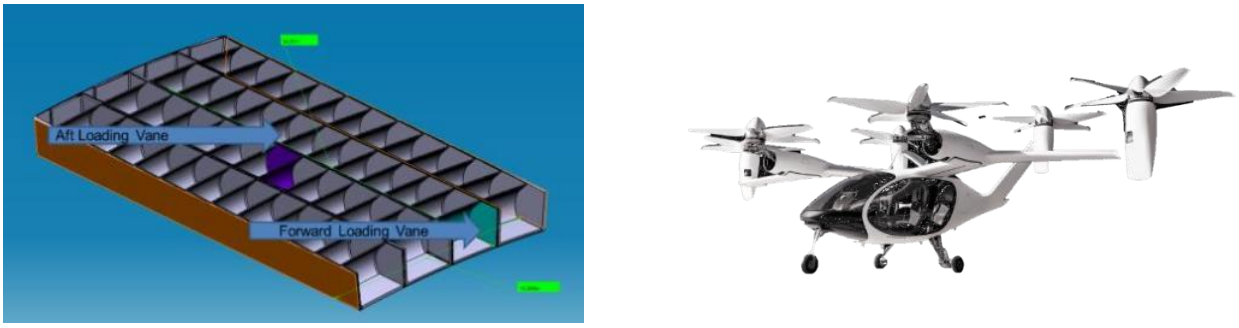

Candidate parts for TuFF forming demonstrations from Spirit (left) and the door frame on the Joby UAM vehicle (right).

Spirit Reverser Cascade

The cascade is an assembly of several vanes, of which there are two types as shown in in the figure. There are 1200 vanes per twin-engine aircraft with 600 of each type. A nominal production rate of 100 aircraft/year leads to a volume of 120,000 parts per year production. Forming assessments are initially focusing on the Forward Loading Vane (left image), to be followed by the Aft Loading Vane (right image).

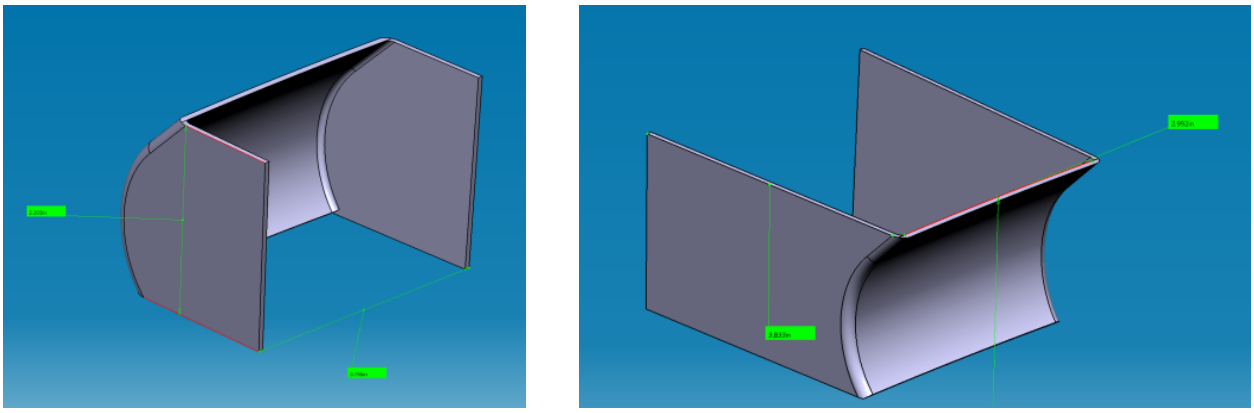

Forward and Aft Loading Vanes from the reverser cascade assembly. Part sizes are approximately 4" (height) x 3" (wide) x 2.5" (deep).

Forming process development for the Forward Vane focused on geometry-based strain calculations to develop processes to keep within the 40% strain limit for *TuFF*. Several forming process variants will be evaluated including stretch forming, drape forming and bladder molding. Initial process trials will use an isothermal low rate forming process to reduce the number of process variables and used to validate blank holding strategy and boundary constraints, tooling design, forming rates and post-formed part characterization. Spirit has provided Vane requirements in the form of laminate design, target thicknesses, geometric tolerances across key features and surface finish.

A modular forming tool and blank holding system has been designed and is currently being fabricated at CCM, with the CAD assembly shown below. The system is designed to be implemented in our hydraulic press with heated platens for the initial set of isothermal experiments and can me subsequently modified for high rate forming experiments. The initial set of experiments focus on the bottom curvature of vane and process conditions to form high quality with the desired curvature in both directions.

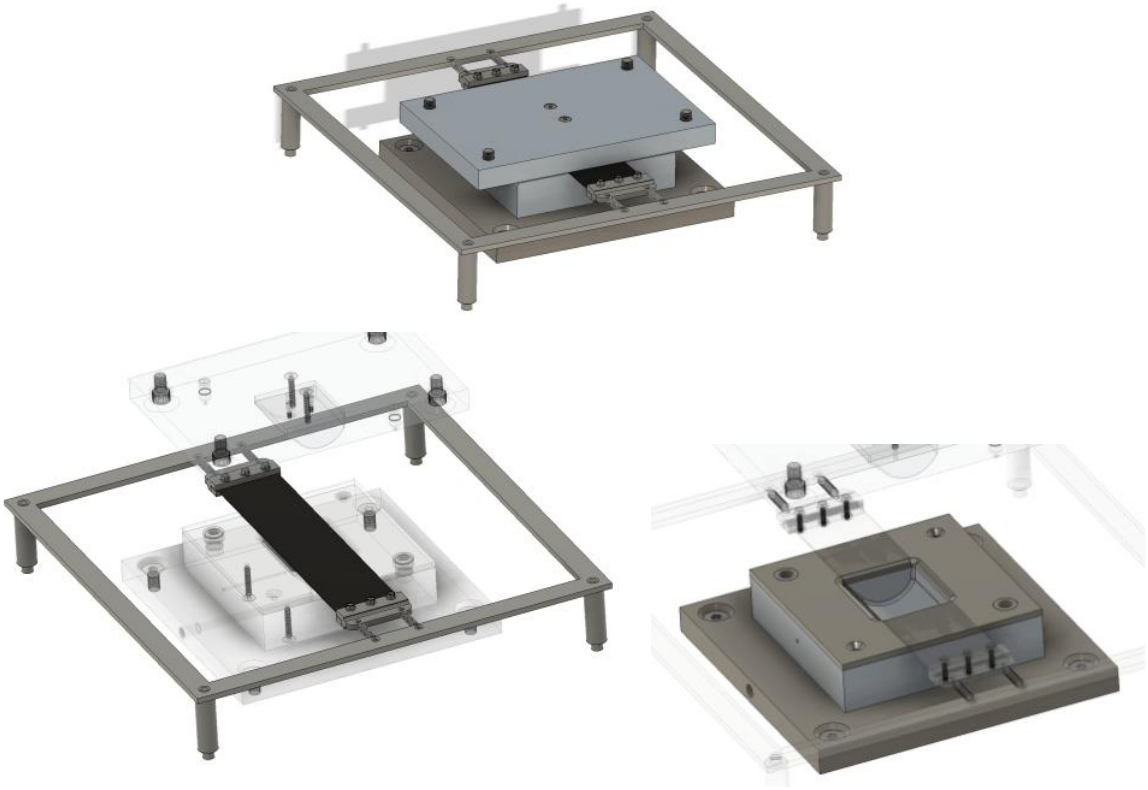

Forward Loading Vane forming demonstration tooling (in production). Top image shows the fully assembled tooling, lower left shows the blank holder design and lower right shows the Vane lower section tool to evaluate formability.

Joby Door Frame

Discussions with Joby on candidate parts relevant to their current air vehicle, led to the selection of the door frame component shown below. This is a complex geometry part with both local feature changes as well as global double curvatures that is currently being fabricated by hand layup. Current production process involves complex ply patterns to account for geometry, full part debulking every two plies during the layup process, followed by autoclave cure. Program goals are to evaluate door manufacturability using *TuFF*'s stretch capability and establish improvements in simplifying ply patterns, reducing debulking frequency and improving manufacturing throughput/cost.

Joby has provided all necessary baseline data including door frame CAD files, laminate schedules for the current design, ply patterns for the door based on the fabric prepreg in use and shipped the female half of the door frame tool shown to CCM for forming trials.

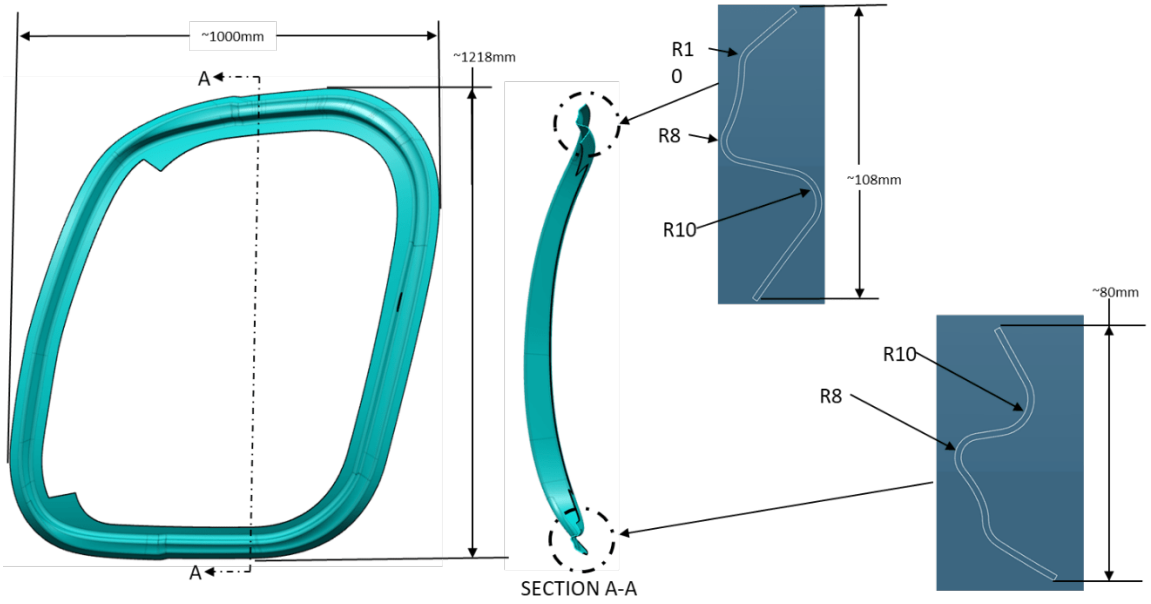

Door frame component drawing from Joby Aviation, selected as the candidate demonstration part, with cross-section complexity at key locations on the door frame.

Process trials are in progress with *TuFF*/thermoset prepreg, based on 3mm IM7 fibers and Axiom 5201 epoxy resin as these trials can be performed at a relatively low temperature (50 C) to demonstrate formability in the large tool. Trials will be conducted in sections to demonstrate gains in manufacturability (forming into geometry, increased thickness per debulk), followed by combining of multiple sections into a single formable preform. Results from these trials will guide the overall door frame manufacturing concept prior to full-scale part demonstration.

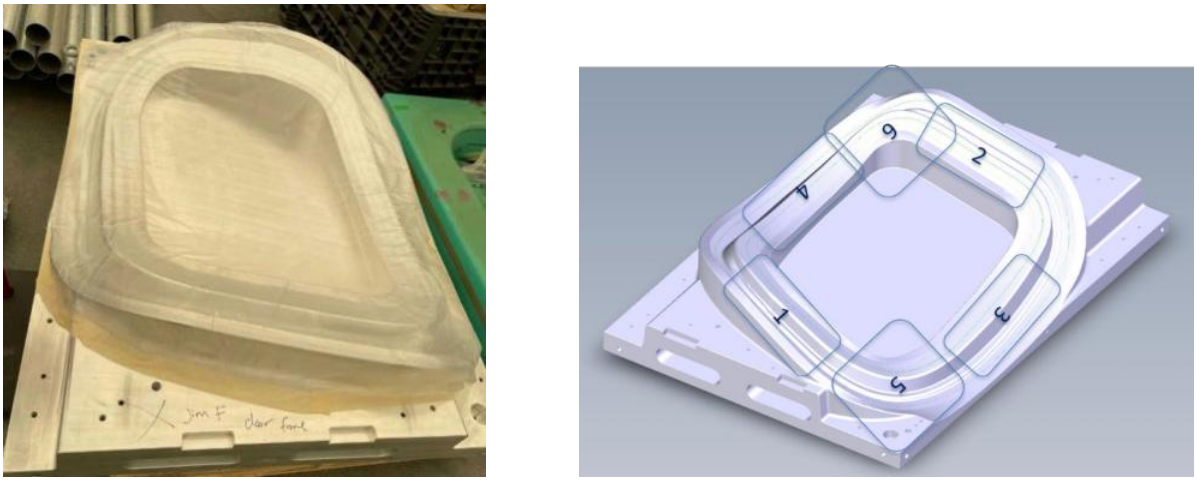

Joby Door frame tool at UD-CCM (left), door frame zones1-6 for preliminary formability assessment (right).

Process trials are in progress with *TuFF*/thermoset prepreg, based on 3mm IM7 fibers and Axiom 5201 epoxy resin as these trials can be performed at a relatively low temperature (50 C) to demonstrate formability in each zone. A Joby engineer completed a site visit (August 8-10, 2022) at UD-CCM and forming trials for zone 1 were conducted during the visit. The first trial below

shows an example of a successful forming demonstration of a 4-ply cross-ply prepreg stack formed into zone 1. Forming trials will continue with increasing thickness, followed by trials for zones 2-6.

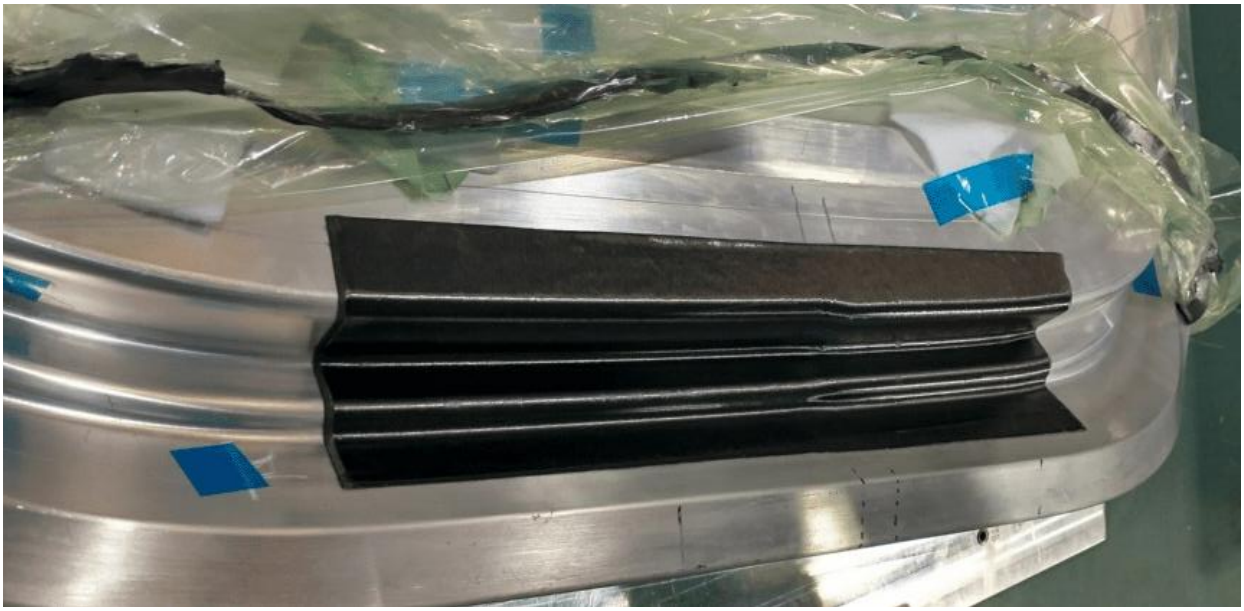

Successful first trial on Joby door frame: 4 layer cross-ply 3mm IM7 TuFF prepreg fully formed into zone 1 of the door frame tool. All key features including the local joggle were fully formed. Forming trials were conducted with Joby engineer on site.

Self-Healing Composites (Southern University)

Evaluation of the interfacial shear strength and self-healing of IM7/vitrimer single fiber composites

A shape memory vitrimer (SMV) composed of Diglycidyl 1,2-cyclohexanedicarboxylate (DCN) and a low molecular weight branched polyethyleneimine (PEI), molecular structures shown in the figure below has been identified as a potential self-healing composite matrix for use with *TuFF* for UAM applications. In a work by Feng and Li in 2021, room temperature self-healing after a low-velocity impact was shown to be effective on continuous fiber-reinforced composites at the laminate scale to heal delamination. In this task, the feasibility to heal fiber matrix interfaces in short fiber-reinforced *TuFF* composites is investigated. This interface plays an important role in both composite performance in both quasi-static and fatigue loading since it dictates the load transfer efficiency amongst the fiber reinforcements. Thus, it is important to evaluate the interfacial shear strength (IFSS) of a composite on the micro level to reflect the properties on the macroscopic scale. Therefore, a collaboration between Southern University and the University

of Delaware Center for Composite Materials (UD-CCM) through a summer visit by a Southern University graduate student (Obed Tetteh) to UD-CCM. The work is focused on investigating the fiber/matrix interfacial bonding strength and the vitrimer's potential for healing interfacial debonding.

Initial efforts were made to determine the appropriate formulation that can achieve a glass transition temperature (T_g) high enough for structural applications. Different monomer feed ratios were mixed and characterized using a DSC to determine the glass transition temperature (T_g) for the various formulations. The T_g plateaued at approximately 90°C starting around a DCN:PEI ratio at 3:1, as shown below. It must be noted that as the T_g is increased, intrinsic room temperature healing may not be observed and *vice versa*. Since the original work by Feng and Li was on a different formulation with a lower T_g, self-healing tests were necessary to determine self-healing process window and effectivness to regain interfacial shear strength.

Though there are four different fiber/matrix interface characterization techniques, not all are suitable for different resins. A single fiber pullout test was selected for the interface characterization and planned interface healing experiments. Rheology was conducted on this DCN:PEI = 3:1 system to determine a partial cure cycle to gel the resin and stabilize the fiber pullout sample during preparation. The figure shows a sample being prepared with unsized IM7 carbon fiber.

Single fibre pull-out tests were performed on the as-fabricated IM7 composites with a DCN:PEI ratio of 3:1. The effective IFSS was found to be 109 MPa which is exceeds the minimum IFSS requirement for property translation in *TuFF* composties (a minimium of 50-60MPa is needed). Additionally, it must be noted that intrinsic room-temperature self-healing may not be visible at 3:1 ratio, and thus the composites must be heated below the glass transition temperature and pressurized to heal any damage that may occur in real-life applications.

Self-healing of the IM7/vitrimer interface will be conducted in the coming year. Samples with a fiber embedded length of 40 μm will be tested until debonding. The debonded length will be measured between the meniscus and resin with a microscope. Samples will be allowed to self-heal over different lengths of time. After healing, the composites will be tested till pullout or just debond and the debonded length will be substracted for conventional data reduction.

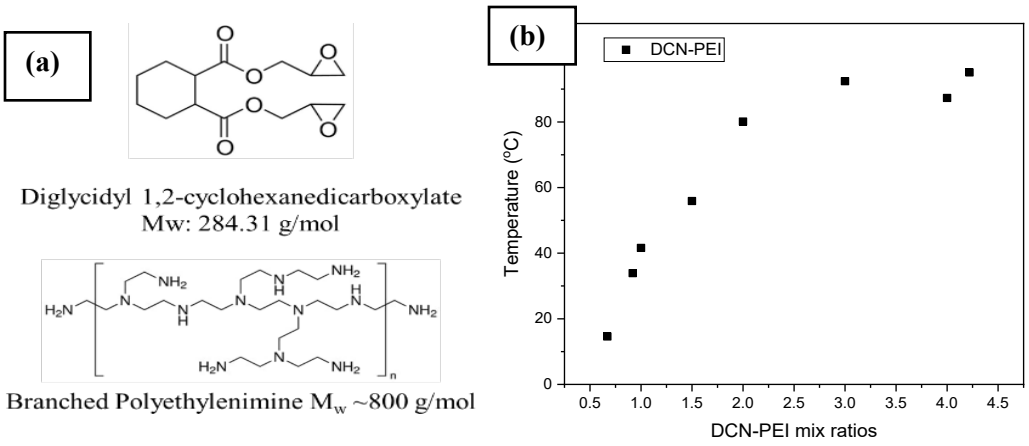

(a) Chemical structure of DCN and PEI; (b) T_g vs monomer feed ratios

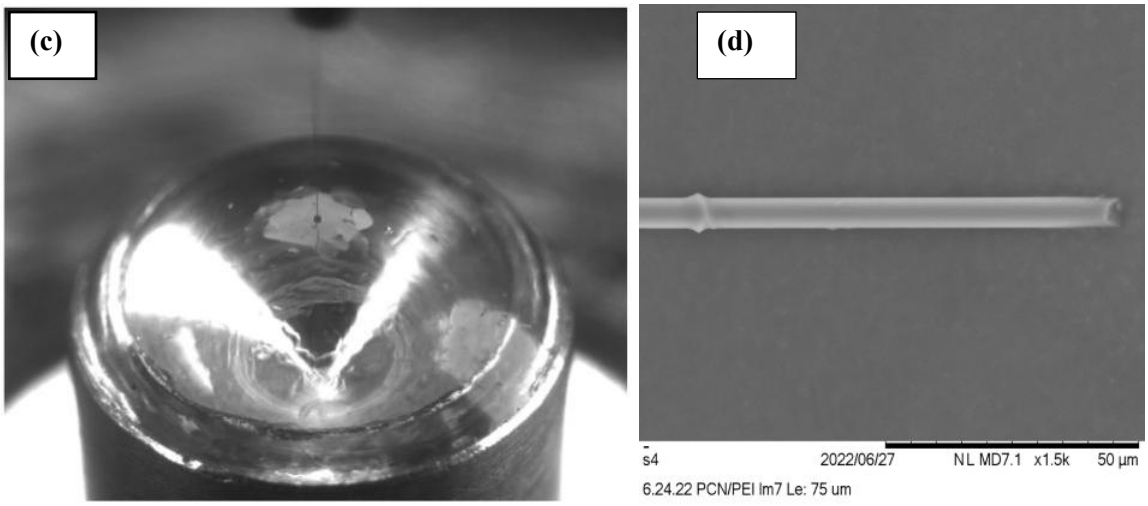

(c) Fiber pullout sample being prepared; (d) SEM micrograph of the composite sample after pullout testing

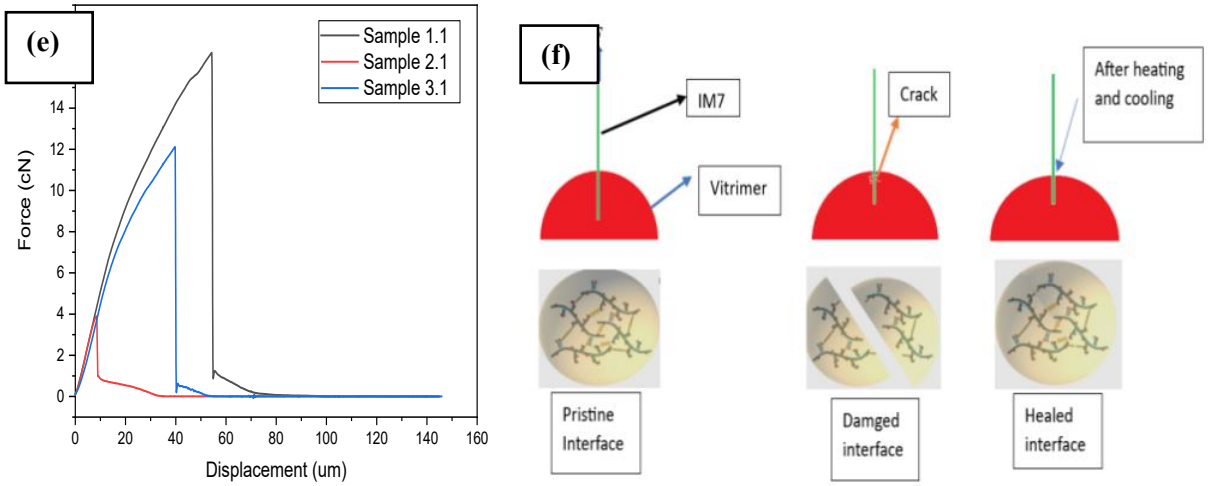

(e) Force-displacement curves of IM7/DCN-PEI sample from a fibre pull-put test and
(f) Schematic of the healing process of the IM7/vitrimer interface with healing mechanism

Papers/presentations

1. Featured Speaker Shridhar Yarlagadda, "Highly-aligned Discontinuous Fiber Composites (*TuFF*): Progress and Challenges, May 23-26, SAMPE 2022, Charlotte, NC.

2. Featured Speaker John W. Gillespie Jr., Nasa ULI Tech Talk Series, "Composite Manufacturing Technologies for Aerospace Performance at Automotive Production Rates", April 18, 2022.

3. Nasa ImaginAviation, March 1-3, 2022, ULI-Aerospace Performance at Automotive Rates Featuring the University of Delaware with Taka Kubota (MSE PhD) and Steve Crimaldi

4. Nasa ImaginAviation, March 1-3, 2022, Student Sustainability Roundtable Imagining a Greener Future Featuring the University of Delaware with Uday Balaga (ME PhD) and Taka Kubota (MSE PhD)

5. Parambil, Nithin K., Chen, B., Deitzel, J., Gillespie, Jr., J.W., "A Methodology for Predicting Processing Induced Thermal Residual Stress in Thermoplastic Composite at the Microscale", https://doi.org/10.1016/j.compositesb.2021.109562, *Composites Part B*, volume 231, 109561, 2021.

6. Simacek P., Advani S. G., Gillespie Jr. J. W., "Modeling Short Fiber Deformation in Dilute Suspension: Fiber Deposition", https://doi.org/10.1016/j.compscitedh.2021.109149, Composites Science and Technology, volume 218, 109149, 2021.

7. Cender, Thomas A., Fidlow, H., Yarlagadda, S., Heider, D., Simacek, P., Advani, S.G., Gillespie, Jr., J.W., "Forming Limits of *TuFF* Composites in Stretch Forming Processes", SAMPE 2022, Charlotte, NC, https://www.nasampe.org/events/EventDetails.aspx?id=1244904, May 23-26, 2022.

8. Fidlow, H., Cender, T. "Extensional Viscosity of Thermoplastic Composites in Stretch Forming Processes", SAMPE 2022, Charlotte, NC, May 23-26, 2022.

9. Chen, Branndon R., Prakash, K., Yarlagadda, S., Gillespie, Jr., J.W., "Fatigue Performance of Thermoplastic *TuFF* Composites", SAMPE 2022, Charlotte, NC, https://www.nasampe.org/events/EventDetails.aspx?id=1244904, May 23-26, 2022

10. Fussel, Lukas, Cender, T.A., Austermann, V., Gillespie, Jr., J.W., Heider, D., "Tow Steering of Stretchable *TuFF* Thermoplastic Tape with Laser Tape Placement", SAMPE 2022, Charlotte, NC, https://www.nasampe.org/events/EventDetails.aspx?id=1244904, May 23-26, 2022

11. Abu-Obaid, Ahmad, Ganesh, R., Gillespie, Jr., J.W., "Investigation of Size and Spatial Distribution of Defects in S2 Glass Fibers Using Continuous Bending Test Method", SAMPE 2022, Charlotte, NC, https://www.nasampe.org/events/EventDetails.aspx?id=1244904, May 23-26, 2022

12. Parambil, Nithin K., Chen, B.R., Deitzel, J.M., Gillespie, Jr., J.W., Vo, L.T., Sarosi, P., "Predicting Processing Induced Residual-Stresses in Carbon-Fiber-Thermoplastic Micro-Composites", ASC Conference, Virtual Event, https://na.eventscloud.com/website/17366/, Sept. 19-22, 2021.

13. Chen, Branndon R., N.K. Parambil, J. Deitzel, J.W. Gillespie, Jr., L.T. Vo, P. Sarosi, "Interfacial Shear Strength (IFSS) and Absorbed Energy versus Temperature in Carbon Fiber-Thermoplastic Composites via Single Fiber Pullout Testing," ASC 2020, https://asc2020nyc/ September 14-17, 2020

Education/Workforce Training and Outreach Activities

During the past year, we have been very active in education/workforce training and outreach to involve students including underrepresented minorities in composites activities at UD and SU. Overall, approximately 550 students (60% were URM from grades K-12) were involved

and more than 450 people registered for presentations and seminar. The activities have been posted on our website and social media outlets providing wide-spread visibility to the composite's community.

In addition, more than 1000 people in total registered for the NASA ImaginAviation Annual Conference and NASA Tech Talk Seminar series that highlighted our ULI students and technical activities.

UD-CCM Education/Workforce Training and Outreach Activities

- Recruitment of UD student for NASA Fellowships through our College of Engineering and UD's university wide Honors program.
- The ULI co-sponsored 9 research reviews (32 talks in total) from March 10th through May 19th, 2022. The reviews typically included 3-4 talks and were attended by 30-50 people from the university and industry. Posted on website (presentations and videos) https://www.ccm.udel.edu/research/research-reviews
- Our ULI co-sponsored Mr. Chris Pederson, President of Specialty Engineered Materials, Avient Corporation to present a talk on keys to a successful career in the composites industry at our annual Student Achievement Day on May 6th, 2022, to students, staff, faculty, and external participants entitled. The talk was well attended (more than 60 participants) and provided valuable advice on professional development and career advancement.

- Our ULI co-sponsored our Summer Research Symposium on August 12th, 2022, with over 50 attendees. The symposium included 28 students (short presentations and poster sessions) from UD-CCM including 3 from Newark Charter high school.
- Our ULI sponsored two Senior Design projects in UD's Department of Mechanical Engineering in the Fall of 2021 to design and fabricate blank holder for forming *TuFF* composites and design and fabrication of high throughput spill ways for fiber alignment. Each project involved 4 seniors advised by ULI co-PIs.

- Our ULI sponsored the Delaware Aerospace Education Foundation – UD Summer Camp 2022 Destination Moon – Space Beam Challenge on July 12-14th.

  Thirty-Eight (38) students entering 7th, 8th and 9th grade attended UD Destination Moon summer camp. The camp integrates real world experiences with Lunar Studies, lessons in Development, Advanced Rocketry, Remote Sensing, Robotics, Computer Sim,

Composite Materials & Telescope Building along with Field Trips.
https://www.dasef.org/aerospace/over_night.htm

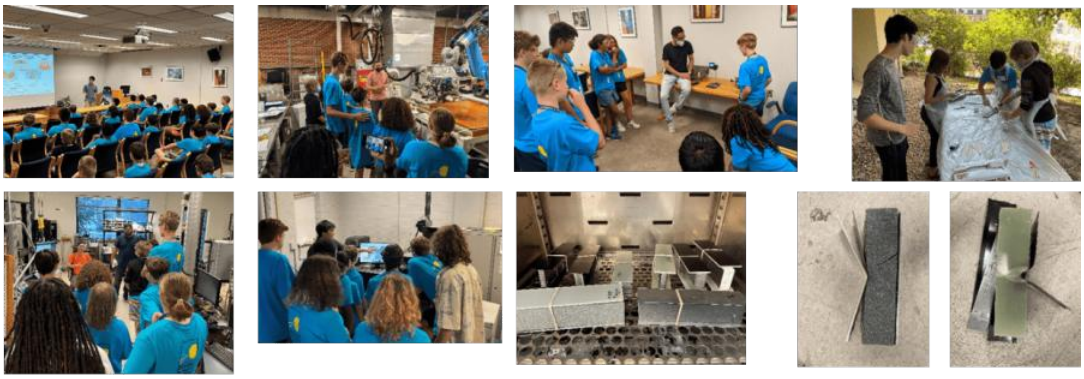

Co-Sponsored By

Southern University Education/Workforce Training and Outreach Activities

In year-two of the *TuFF* ULI project, Southern University engaged in several education/workforce training and outreach initiatives by leveraging SU's CREST Center for Multifunctional Composites education and outreach program activities for underrepresented minorities. The activities are listed in the table below.

SU K-12 Outreach Activities

Date of Activity	Name of School / Program	Parish	Grades of Participants	Number of Students
09/29/2021	Melrose Elementary School / SUBR CREST/SWE Section Volunteer Activity	East Baton Rouge	3rd – 5th grades, (girls)	30
02/24/2022	Park Forest Middle Creative Sciences and Arts Magnet, 2022 Family Math and Science Night	East Baton Rouge	4th – 8th grades	150
06/03/2022	Southern University Laboratory School Summer Enrichment Program	East Baton Rouge	7th – 12th grades STEM Challenge: Save the Eggstronaut	55
06/14/2022	Southern University Laboratory School Summer Enrichment Program	East Baton Rouge	7th – 12th grades STEM Challenge: Rocket Build	55
06/16/2022	Southern University Laboratory School Summer Enrichment Program	East Baton Rouge	7th – 12th grades STEM Challenge: Rocket Launch	55
06/23/2022	McComb School District	McComb, MS Pike County	6th – 8th grades STEM Day at SU	37

Overall, faculty and students participated in six outreach activities. Figure 1 shows some highlights of some of these activities. In Figure 1 from top left to right and bottom left to right a) Faculty and undergraduate students visited Park Forest Middle school to participate in their Math and Science Night, from 6 to 8 pm. They set up demonstration station for 3D printing of polymer structures using Digital Light Processing 3D printing. b) & c) Southern University Lab School Summer Enrichment Program. Held at Southern University Lab School at SU, June 1 – 30, 2022. d) McComb School District SU STEM Day. Held at SU in Pinchback Hall on June 23, 2022.

Education/workforce training and outreach initiatives at Southern University

SU students supported with *TuFF* ULI funds participated in CREST Center sponsored research education for undergraduate (REU) during fall 2021, spring 2022 semester and in person summer REU programs. Activities included: i) REU projects with graduate student and professors as mentors, ii) weekly virtual and in person professional development seminars with invited guest presenters, iii) Tours and training in SU and Louisiana State University (LSU) laboratories, iv) Poster symposium where student presented research undertaken at the end of fall, spring semester and summer REU programs. Figure shows REU students participating in professional development Seminar. One SU

REU student participating in Professional development in Lab

graduate student visited University of Delaware CCM to engage in training and conducted experiments using CCM thermal/chemical/rheology and mechanical testing equipment as well as our interphase specimen preparation and fiber pull-out testing facilities on vitrimer polymer. The SU student worked closely with CCM staff, students, and technicians during the 2-month internship.

SU graduate student Obed Tetteh working in CCM labs

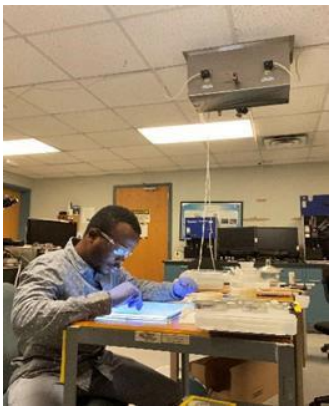

Diversity Data: September 2021 – August 2022

Total Number of PI/Co-I's: 14
- Male: 14 (100%)
- Female: 0 (0%)
- URM: 2 (14%)

Total Number of Universities: 2
Total Number of Industry Partners: 3
Total Number of Students: 79
- Male: 67 (85%)
- Female: 12 (15%)
- ULI Funded: 18
- ULI Unfunded: 61
- Graduate: 21
- Undergraduate: 58
- URM: 13 (16%)
- Postdocs: 2

Other Support Staff: 12
- Male: 6 (50%)
- Female: 6 (50%)

Schedule and Milestones

The program milestones and scheduled are shown below for the 4-year program.

	Year 01				Year 02				Year 03				Year 04			
	Q1	Q2	Q3	Q4	Q1	Q2	Q3	Q4	Q1	Q2	Q3	Q4	Q1	Q2	Q3	Q4
Task 1: Road-Mapping and Requirements																
a) Technology Roadmap for UAM/Aviation																
b) Requirements Definition																
c) Benchmark of Alternative Materials/Processes/Simulation Tools																
d) Feature-Based Part Selection (Non-Proprietary)																
Task 2: TuFF Modeling Tools and Validation																
a) Fiber-scale mechanisms and validation																
b) Ply-scale Mechanics and Forming Process Simulation																
c) Laminate scale models for process/part design																
d) Integrated mechanics-forming and validation																
e) Cost Modeling (from Fibers to Part)																
Task 3: Property Database																
a) Baseline B-basis property characterization																
b) Formed blank property characterization																
c) Post-Formed Properties																
Task 4: Process Development																
a) Hardware Development (Heating, Fixturing, Tooling)																
b) Process Optimization																
c) At Rate Sub-Component Demonstration																
d) Post-Form Validation (Geometry, Properties)																
Task 5: Technology Demonstration																
a) Virtual Process Optimization (Tailored Blank, Tooling, Forming)																
b) At Rate Full-Scale Part Fabrication																
c) QA/QC Meeting Part Specification (Geometry, Properties, Cost)																